International Journal of Impact Engineering 49 (2012) 192–213

Contents lists available at SciVerse ScienceDirect

International Journal of Impact Engineering

journal homepage: www.elsevier.com/locate/ijimpeng

Review

Stress-strain behavior of sand at high strain rates

Mehdi Omidvar [a], Magued Iskander [a,*], Stephan Bless [b]

[a] Civil Engineering Department, Polytechnic Institute of New York University, Six Metrotech Center, Brooklyn, NY 11201, USA
[b] Institute of Advanced Technology, University of Texas at Austin, USA

ARTICLE INFO

Article history:
Received 30 December 2011
Received in revised form
11 March 2012
Accepted 12 March 2012
Available online 21 March 2012

Keywords:
Dynamic response
Impact
Uniaxial compression
Split hopkinson pressure bar
Dynamic triaxial test

ABSTRACT

A review of the response of sand under high strain rate (HSR) loading is presented. The response observed in HSR uniaxial compression tests, split-hopkinson pressure bar (SHPB) tests, and triaxial tests is investigated. Previous monotonic HSR tests have been reviewed, summarized, and combined in order to illustrate the effects of HSR loading on the confined modulus, stress-strain response, and shear strength of sand. The effects of strain rate, initial void ratio, confining pressure, saturation, shape and size of grains, as well as grain mineralogy on the response of sand to HSR loading are also discussed. Issues related to inertial effects that may affect HSR response are explored. A brief summary of the response of sand to shock loading is also presented. The review provides a comprehensive understanding of the important aspects of HSR response of sand, in support of the growing interest in the behavior of sand subject to rapid loading conditions.

1. Introduction

Soil response to high strain rate (HSR) monotonic loading is of interest in the study of many engineering problems including explosions and air blasts [1–3], earthquakes [4], mine blasts [5–8], vehicle and aircraft wheel loading [9,10], dynamic compaction [11], pile driving and rapid load testing of piles [12], and projectile penetration [13–15].

Considerable research has been devoted over the past sixty years to characterization of soil behavior under HSR loading. Numerous investigators have employed conventional geotechnical testing equipment with unique modifications to accommodate rapid load testing, while others have explored alternative methods of testing such as the Split Hopkinson Pressure Bar (SHPB) test and plate impact tests [16–18] in order to achieve higher strain rates. Great progress has been made through pioneering works, and the accumulation of data has lead to a deeper understanding of soil behavior under rapid loading.

This review presents a summary of the various aspects relating to HSR response of sand. A brief review of testing equipment, as well as discussion of fundamental aspects of HSR loading effects in sand is included. The focus of this review is on HSR effects associated with monotonic dynamic loading conditions. The reader is referred to [19,20] for a review of time-dependent behavior of sand involving static viscous effects such as creep and stress relaxation.

2. Behavior of sand under quasi-static loading

In order to investigate the effects of HSR loading on sand, it is desirable to first identify the factors that contribute to the quasi-static response. The behavior of sand is typically studied under uniaxial or triaxial conditions.

2.1. Uniaxial response

Typical static stress-strain response of dry sand under uniaxial (confined) compression over a wide range of stress levels is illustrated in Fig. 1, noting that compressive stress is taken as positive in accordance with soil mechanics conventions. In a uniaxial test a sample of sand is compressed axially while lateral strains are prohibited. There are three main mechanisms governing response of sand in uniaxial compression: (1) elastic compression of individual sand grains; (2) slippage and rearrangement of grains; (3) grain crushing. The three mechanisms occur at different threshold stress levels, and four distinct regions may be identified in the response based on the governing mechanism [21]:

Zone 1: The axial stress level applied in this region is not enough to overcome the kinetic friction between individual sand grains. Stress-strain response in this initial region is elastic, corresponding to the elastic deformation of individual grains.

* Corresponding author. Tel.: +1 718 260 3016; fax: +1 718 260 3433.
E-mail address: Iskander@poly.edu (M. Iskander).

0734-743X/$ – see front matter © 2012 Elsevier Ltd. All rights reserved.
doi:10.1016/j.ijimpeng.2012.03.004

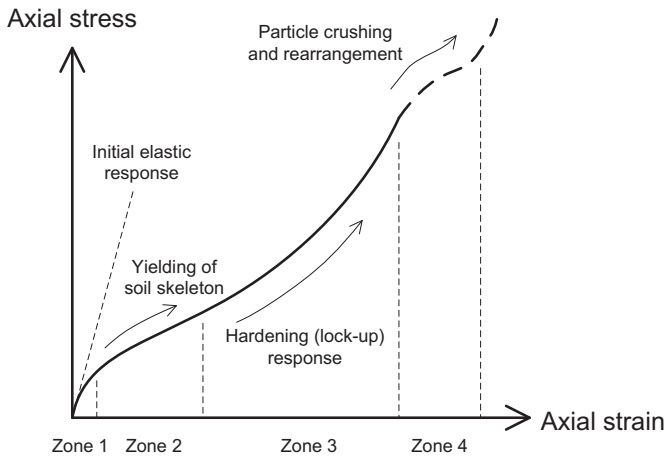

Fig. 1. Stress-strain response of dry sand in uniaxial strain loading under static loading (redrawn per Whitman [21]).

Zone 2: At a threshold range of stresses the applied axial stress exceeds the static friction between sand grains, and the soil skeleton deforms as the grains slide and roll into the voids. The stress-strain behavior in this region is inelastic corresponding to the yielding of the soil skeleton. In metals, yield behavior may result in loss of shear strength but no change in density. However, in soils, deformation of the skeleton results in both shear deformation and compaction [22].

Zone 3: Rearrangement of sand grains into the voids results in a denser arrangement, thereby increasing contact points between the soil grains. Sliding and rolling becomes more difficult, and a hardening response is observed as the particles “lock-up” into a denser arrangement.

Zone 4: At high stress levels individual grains begin to crush, allowing the skeleton to contract further, thereby reducing resistance to compression. This yielding behavior results in an even denser arrangement of particles, and the response eventually shifts once again to a lock up behavior.

The response of sand in uniaxial compression may be quantified in terms of the constrained modulus, *i.e.* the slope of the one-dimensional stress-strain curve at a given strain. There are several factors that affect the stress-strain response, including:

- *Applied stress level:* The uniaxial response of sand may exhibit a yielding behavior or a lock up behavior in stress-controlled tests, depending on the magnitude of the applied stress. At lower applied stress levels a yielding behavior is observed. As the load is incremented to higher stress levels a lock up response may occur [23,24]. De Beer [25] reported similar observations, and added that the compressibility of quartz sand, defined as the inverse of the constrained modulus, decreases as vertical effective stress is increased up to 14.7 MPa, attributed to continuous rearrangement and packing of sand particles into denser arrangement. At higher stress levels compressibility increases due to rearrangement of grains facilitated by grain crushing. De Beer also reported that compressibility eventually decreases again at higher pressures (approximately 34.4 MPa), reasonably attributed to the lock up of particles following crushing and rearrangement into denser arrangement, as indicated in Fig. 1.
- *Initial void ratio:* Loose sand grains have fewer contact points compared to dense sand. Therefore, loose sand will exhibit a yield-type response in a wider range of strains as grains rearrange into the voids [26]. Moreover, under stress-controlled test conditions grain crushing occurs at lower stress levels in loose sand compared to dense sands since there will be higher stresses accumulated at the fewer contact points between sand grains in loose sand compared to dense sand [23], as indicated in Fig. 2. Finally, although initially loose and dense sands lock up at different strains, the initial void ratio loses its effect at high incremented pressures, and void ratios of loose and dense sand approach a similar value. The stress level at which void ratios converge increases with increasing mineral hardness [27–29].
- *Particle size, shape, gradation*, *surface texture and mineralogy*: Studies indicate that grain crushing increases with increase in particle size in uniform sand [30]. Moreover, rounded and sub-rounded grains are less susceptible to grain crushing compared to angular soils due to presence of fewer asperities prone to local stress concentration [31]. Well-graded aggregates compress less, and are less prone to grain crushing compared to poorly graded aggregates [32]. Surface texture also plays a significant role in the response of sand. For example, Horn and Deere [33] and Lee and Seed [44] found that the sliding friction coefficient of partially saturated sand minerals is controlled by surface roughness. Such observations play an important role in the uniaxial compression response of sand, and must be taken into account in explaining experimental observations in HSR loading.

2.2. Triaxial response

Contrary to the uniaxial compression test where the soil is laterally constrained, in a conventional triaxial compression test a constant confining pressure is maintained within the sample. Lateral stress is kept constant and the soil is allowed to deform laterally, allowing it to reach the "critical state" where the soil continuously undergoes shear strain at a sustained shear resistance and under constant void ratio, i.e., without change in volume [34,35]. The triaxial shear test is commonly employed to describe shear strength and stress-strain characteristics of soils.

In critical state soil mechanics the definition of failure can be given in a number of ways including simple Mohr-Coulomb envelopes, or by defining a critical state failure line [35] as depicted in Fig. 3a. Typical mean stress paths and stress-strain response, along with the Mohr circle of stress representation for sand under uniaxial compression and triaxial compression are illustrated in

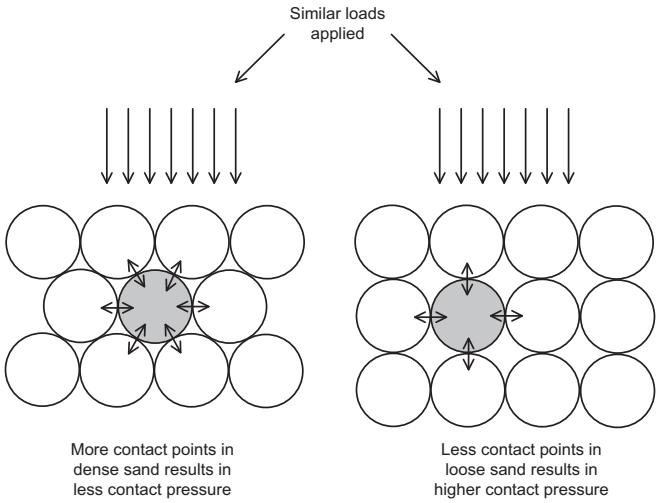

Fig. 2. Comparison of contact points in ideal loose and dense sand in uniaxial compression.

Fig. 3. It can be seen that the triaxial soil specimen approaches failure with a sustained maximum shear stress, whereas the uniaxial specimen deforms without reaching the critical state line. Moreover, it is evident from Fig. 3c and d that although both specimens experience shear stresses, the uniaxial specimen does not reach the critical state, whereas the triaxial specimen fails in shear as defined by the critical state. Intermediate lateral confinement will yield results within the two extreme cases, as discussed by Goh et al. [36]. Finally, shear resistance in sand is not a constant prior to the critical state, but is rather a function of the applied confining pressure and the initial void ratio.

In a conventional triaxial test if the test is performed slow enough such that pore water pressure is not permitted to build up, the test is termed a *drained test*. Drained tests are typically representative of the behavior of *in situ* sand subject to static loading due to high hydraulic conductivity of sand. Shear strength of sand under drained static loading is a result of inter-particle forces, governed mainly by three mechanisms that contribute to the friction angle: kinetic friction, rearrangement and dilation, and grain crushing. Kinetic friction, φ_μ, also referred to as sliding friction or inter-particle friction [37], which is the intrinsic component of friction resisting sliding between individual sand grains in the direction of shear, has the dominant contribution at all confining pressures and void ratios. It can be seen from Fig. 4 that φ_μ is relatively independent of the initial relative density and confining pressure, except in very loose sands in which the inter-particle friction may not be fully mobilized [37,38], or at very high pressures, which may result in slightly lower sliding friction [37,43]. Inter-particle friction is controlled by surface roughness, strength, hardness and texture of individual grains, and is in the range of 22°–35°, 31°–34°, and 36°–38° for quartz, calcite and feldspar, respectively [37].

Individual grains do not generally move in the direction of shear, and the mobilized friction angle, φ' may be higher than the inter-particle friction angle. The two mechanisms contributing to the mobilized friction angle are geometric interference and grain crushing, neither of which are intrinsic soil properties. That is, they are affected by loading conditions and initial density, and their contribution to shear resistance may change as these conditions change. Geometric interference is manifested by two mechanisms: pushing and rearrangement, and rolling and climbing of grains also termed dilation due to the volume change associated with this mechanism. The contribution of each of these components depends on the initial void ratio and the confining pressure, as suggested by Fig. 4. At low initial confining pressure, shearing of dense sand is accommodated by geometric interference. Grains are allowed to rearrange and dilate against the applied deviatoric stress, thereby increasing the resistance to shear. As confining pressure increases, geometric interference is restricted and it becomes increasingly difficult for grains to climb (dilate) and push (rearrange) to accommodate shear. Restricted grains therefore crush as they are pushed by adjacent grains to allow for shear to occur. Grain crushing absorbs energy, and therefore an increase in shearing resistance is associated with crushing at higher confining pressures. Lee and Seed [44,45] reported that even though the contribution of dilation to friction angle diminishes under high confining pressures, the friction angle still remains higher than kinetic friction due to the increase in energy absorption associated with particle crushing.

The existence of a stress range below which dilatancy contributes to shear strength, and beyond which particle crushing according to Vesic and Clough [46] becomes "the only contributing factor in addition to kinetic friction", has been established by other authors as well [47–49]. These studies also point out that at confining stresses below breakdown stress, where geometric interference contributes to shear resistance, the initial void ratio and angularity of particles are important, since the magnitude of dilation is controlled by these factors. Recently, separating the effect of interlocking as an independent contributor to the mobilized friction angle was suggested, as shown in Fig. 4. Guo and Su [41] observed that interlocking is much more significant in angular sand compared to round sands. Moreover, it can be seen from Fig. 4 that interlocking significantly contributes to shear strength in dense sand, and under low confining pressures, and loses significance as confining pressure increases. At stress levels beyond the breakdown stress shear strength is no longer related to the initial void ratio, and particle shape, size and mineralogy become more significant [30,48–52]. Accordingly, grain crushing in shear

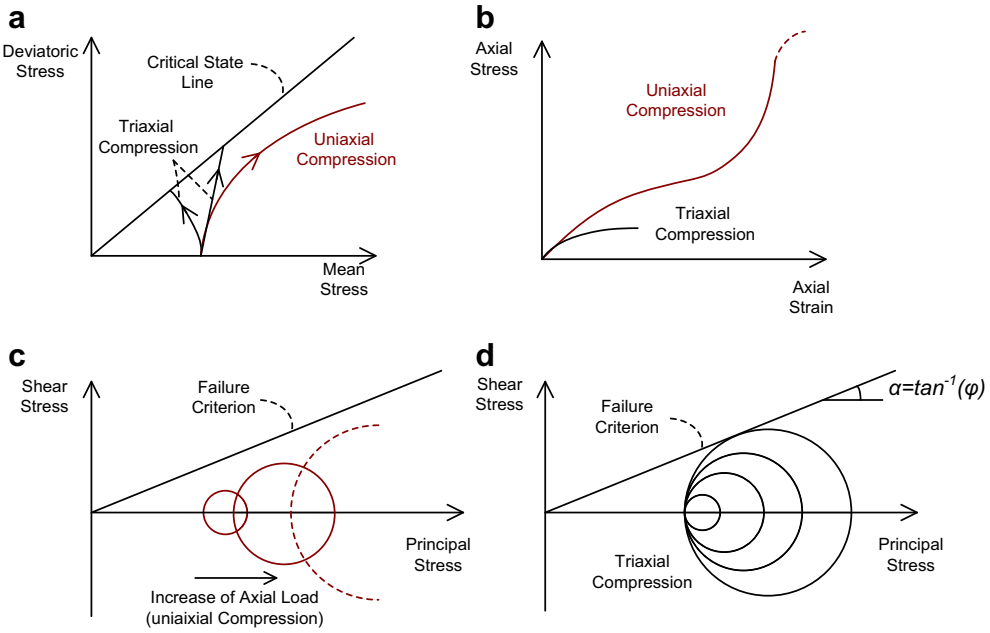

Fig. 3. Comparison of uniaxial compression and triaxial compression response of dry sand, under static loading; a) Stress paths, b) stress-strain response, c) Mohr circle for uniaxial compression, d) Mohr circle for triaxial compression.

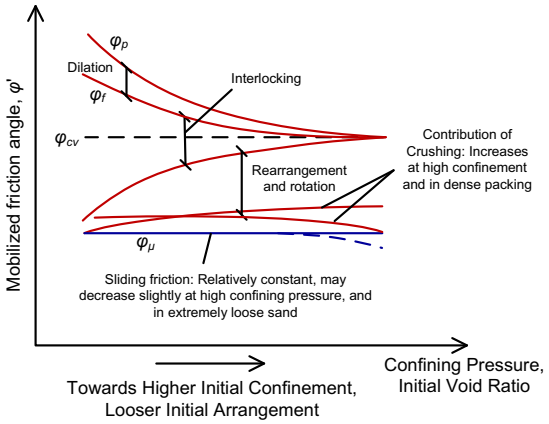

Fig. 4. Components of shear resistance in granular materials based on Stress-dilatancy theory [39,40], along with recent contributions of Guo and Su [41]. φ_μ, φ_{cv}, φ_f and φ_p are interparticle friction angle, constant volume friction angle, friction angle corresponding to the onset of dilation, respectively.

increases with increase in grain size, angularity, uniformity of grain distribution, initial porosity, and is directly affected by the strength of individual particles [53]. Structural weaknesses in larger grains due to possible presence of more flaws and anomalies in individual grains can lead to more crushing in coarse grains compared to finer grains [54–56]. Recent studies suggest that crushing in coarse angular grains under shear consists of shearing-off of asperities, whereas finer grains fracture along their natural cleavage planes [52]. Moreover, stress concentration on individual grains plays an important role in damage and grain fracture, and has been studied by several authors [54,56]. The coordination number, defined as the average number of contacts per grain [57], is used to quantify stress concentration. It has been shown that coarse sands surrounded by finer particles have high coordination numbers compared to fine grained sands. In this case, the tensile stress on coarse grains is smaller compared to finer grains, and coarse grains become less susceptible to grain fracture compared to finer grains [52,56–59]. At any rate, definitive description of individual grain effects relating to particle crushing requires micromechanical observation of the mechanisms involved in the phenomenon during shear, which are limited at this time.

The effect of initial void ratio on friction is depicted in Fig. 4. It can be seen that at small void ratios geometric interference is dominated by dilation, which can contribute up to 30° to the mobilized friction angle under very low confining pressures. The contribution of interlocking is also highest in dense sand, and is particularly significant in angular sands [41]. As the initial void ratio increases, contribution of dilation and interlocking decreases and geometric interference is dominated by grain rearrangement in the greater number of voids available [42]. At the critical state the contribution of dilation and interlocking have diminished as the initial arrangement has been locally destroyed due to severe shearing displacement along the failure plane, which implies that the initial void ratio does not affect the shearing resistance at the critical state, and both initially loose and dense sand show similar resistance to shear at the critical state.

The net result of the contributing components of shearing resistance at different confining pressures and void ratios can be identified on stress-strain curves shown in Fig. 5 using data reported by Lee [61]. The stress axis is expressed in terms of the principal stress ratio, implying that although samples at different confining pressures converge to a similar principal stress ratio as they approach the critical state, they do so at different deviatoric stress levels. Fig. 5 confirms that at very low confining pressures both loose and dense sand show a dilative response, and that the magnitude of dilation is much greater in dense sand compared to loose sand. As confining pressure increases, the response of loose sand shifts to a contractive behavior which persists over a wide range of confining pressures, and increases in rate at higher confining pressures. Dilative response is observed in dense sand under low confining pressures, while the increase in confining pressure reduces the magnitude of dilation. At high confining pressures dilation is restricted, and the response of dense sand also shifts from a dilative behavior to a contractive response. It is also evident from Fig. 5 that at high confining pressures, the peak stress ratio associated with the maximum rate of dilation diminishes as volume expansion is restricted by the confining pressure.

Due to the importance of the above factors, on the observed response of sand, it is important to achieve consistent density and grain size distribution in testing of sand. Therefore, attention to sample preparation methodology under both quasi static and HSR loading is extremely important in order to achieve consistent and repeatable results.

3. Testing of sand for HSR behavior

There is a conceptual difference between an HSR test and a static test. In a slow test as the sand fails, it is allowed to form shear bands, and rearranges itself as stress is measured. In an HSR test, on the other hand, the sand is flowing during the experiment, and has not ceased to flow by the time measurements are made. Viscous flow occurs as the strength of the material is exceeded; the greater the overstress, the greater the strain rate of the viscous flow. Therefore, there are two aspects of the strain rate effect that should be distinguished in the interpretation of an HSR test. The first effect occurs when the strain rate imposed on the specimen boundaries increases, forcing failure to occur in the sample. This may trigger a different mechanism of failure than what would otherwise occur in a slow test. The second aspect of the HSR effect concerns the stress level, particularly in stress-controlled tests. As the magnitude of the HSR stress is increased, viscous flow is forced to occur, and the flow rate depends on the stress level. In the latter, the cause and effect are reversed, and it is the magnitude of the overstress that determines the strain rate observed.

The application of an impact stress to a soil mass introduces a complex stress wave propagating in the soil. Depending on the location with respect to the point of application of the impact loading, the surrounding soil may be affected by a compressive stress wave, a shear stress wave, a Rayleigh stress wave, or a combination of these stress waves. The stress state is more complicated near the ground surface. Stress waves produced by an impact load are typically characterized by fast rise and fall times, high amplitude, and a short duration. The study of the response of soil to HSR loading is commonly carried out in the laboratory using one of the following two concepts:

- Reproducing the stress conditions at the propagating front, by applying a uniform stress throughout a small soil sample to represent the soil affected by the wave front.
- Generating a stress wave and allowing its propagation through a longer soil sample, and studying wave propagation characteristics to derive the HSR response.

Common testing methods based on the above concepts may be divided into four main categories: (1) Uniaxial compression tests, also referred to as confined compression or oedometer tests, (2) Split Hopkinson Pressure Bar (SHPB) tests, (3) Triaxial compression and direct shear tests, and (4) Plane wave shock tests.

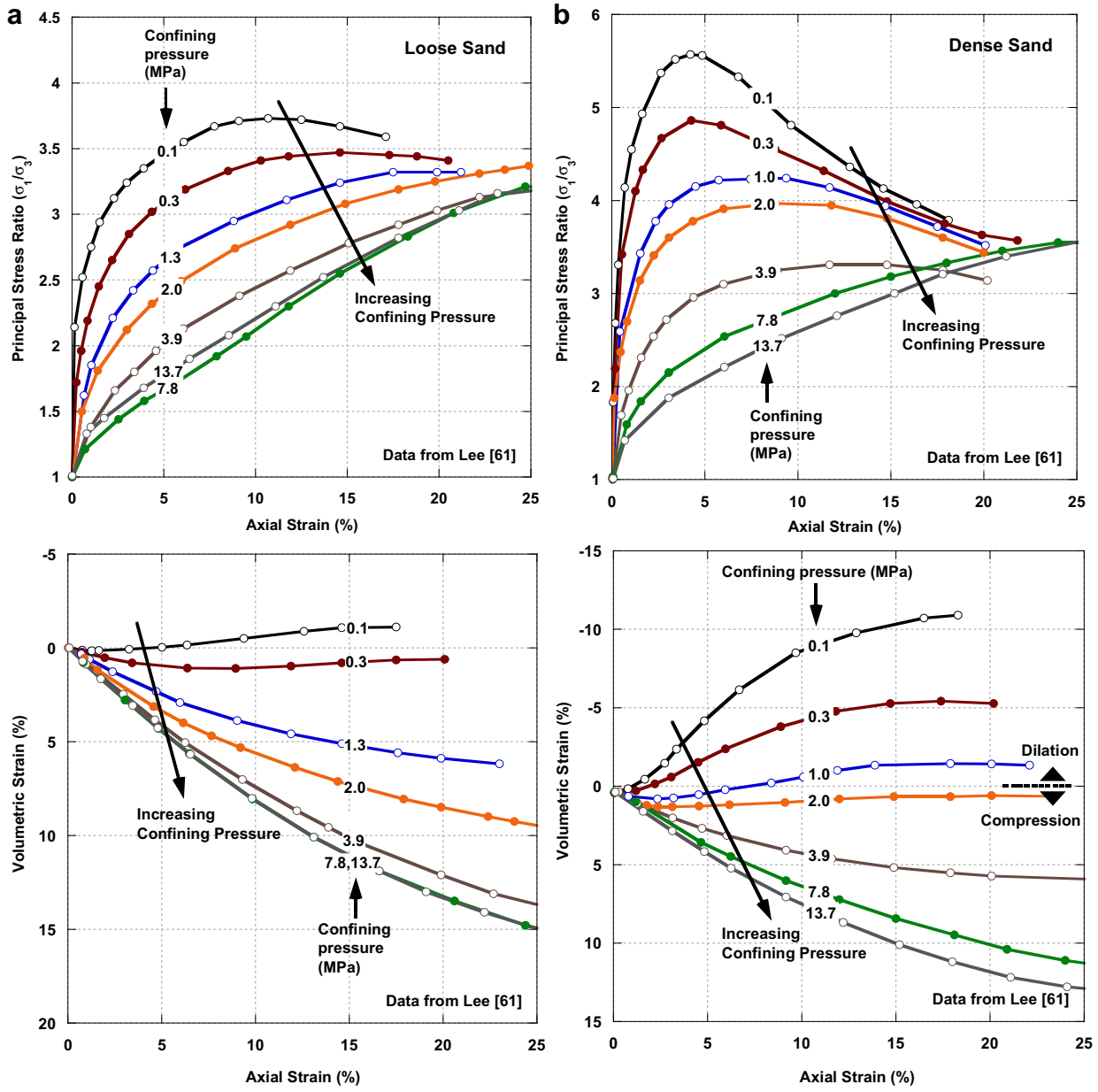

Fig. 5. Effect of confining pressure on stress-strain response and volumetric strain of sand in triaxial compression, under static loading; a) Loose sand, b) Dense sand.

In geotechnical engineering, wave propagation tests rely on monitoring time histories of stress wave propagation through the soil sample to derive the stress-strain response. The method has three main drawbacks [62]: (1) a long soil specimen is usually required so that the stress wave can be monitored as it propagates through the specimen, without complications introduced by multiple reflected waves. Preparing such long specimens is difficult, (2) a long, slender specimen amplifies undesired boundary effects due to sidewall friction [63]. Measures employed to reduce friction typically allow for some lateral strains to occur, thus violating uniaxial compression. (3) Most conventional instrumentation techniques involve intrusive measurements by means of embedding strain gauges in the soil specimen, which may lead to compliance errors. Although several authors have largely overcome this drawback by placing the strain gauges on the outside wall [64,65], the majority of the available soil dynamics literature involves embedded instrumentation for such tests. Due to the aforementioned drawbacks, use of wave propagation tests is usually limited to measuring wave propagation speed and attenuation characteristics, rather than study the stress-strain response.

Despite the aforementioned drawbacks, shock tests which are a particular form of wave propagation tests have been successfully employed to derive stress-strain characteristics of soils under very high strain rates and high stress magnitudes. This review is focused mainly on the stress-strain response of sand obtained from uniaxial compression tests, SHPB tests, and triaxial compression tests. A brief review of shock tests is also provided in order to demonstrate the usefulness of such tests in deriving stress-strain characteristics of soils.

4. HSR uniaxial compression (oedometer) tests

Uniaxial compression tests were originally developed for the study of uniaxial compression of cohesive soils. Use of oedometers

to test sand is also widely documented in the literature [23,31,32]. HSR testing with the oedometer involves application of an impact stress instead of a static load to the cross section of a thin cylindrical soil sample. Impacts are generated by several means including drop weight systems [66], gas-driven pistons [67–70], hydraulic-driven pistons [21,26] and explosive-loaded pistons [71,72]. A summary of HSR uniaxial compression tests from the literature is presented in Table 1.

4.1. Wave propagation effects

The most important consideration in uniaxial compression testing of sand under HSR is to ensure uniform stress distribution within the sample. Immediately after the impact load is initiated on one end, the different stress conditions of the two ends of the soil specimen cause a stress gradient to be established, and a stress wave propagates through the soil as a result. Until several reverberations have had time to occur, the stress is non-uniform in the sample. Consequently, stress-strain curves which rely on average strain will not be accurate. In order to overcome this problem, two general approaches have been suggested: (a) Reducing the thickness of the sample so that the wave travel time in the sample comprises only a fraction of the duration of the applied stress wave; and (b) Control the rise time of the applied impact stress, so that the induced stress wave propagates through the specimen and reflects back and forth many times before the impact stress is fully applied to the specimen. As a result, a relatively uniform stress distribution will be established within the length of the specimen, and global measurements of stress and strain can be obtained.

The former approach has been employed in early HSR tests. Heierli [66] suggested that the thickness of the specimen be limited to about one tenth of the wavelength of the impact stress wave. Although Heierli reported successful application of the method, it is evident that an impact load with a very short rise time would result in a very small, and in some cases impractical specimen thickness. The second approach was first suggested by Whitman [73], and has been widely adopted in the literature.

4.2. HSR effects on confined modulus

The two governing mechanisms in uniaxial compression response, that is, slippage and rearrangement of particles, and particle crushing are both sensitive to the rate of application of the axial load. A comparison of static and HSR uniaxial compression test on dry sand is shown in Fig. 6. Test results from Akers [74] are also depicted in Fig. 7, in which the stress axis has been presented in logarithmic scale (Fig. 7b) in order to magnify the small strain effects shown in Fig. 7a. At the early stages of loading the static and HSR tests have a similar stiffness as evidenced by the common initial tangent in Figs. 6 and 7b. At approximately 1% strain in Fig. 7a, the HSR test begins to exhibit a higher stiffness, as there is less opportunity for the particles to rearrange compared to static loading. At higher stress levels, there will also be less particle breakage under HSR loading compared to static monotonic loading, since particle crushing is a time-consuming phenomenon [43,74–76]. The result is a stiffer response in the HSR test. Moreover, if the load is sustained after application of the HSR load, there is a creep type response in the HSR test as the particles begin to crush with time, as evidenced by the HSR tests shown in Fig. 7.

The dynamic modulus ratio, defined as the ratio of the constrained modulus under impact loading to the constrained modulus under static loading, is employed to quantify the effect of HSR loading on stress-strain response of sand. Results of uniaxial compression tests from several authors have been summarized in Fig. 8, confirming that there is a general, though modest, increase in constrained modulus of sand as a result of HSR loading. However, there is considerable scatter in the data, owing to variations in test conditions, difference in mineralogy, gradation and initial void ratios of the sands employed by different authors, and unaccounted inertial effects. For example, it has been shown that the presence of fines in sand reduces the dynamic modulus ratio [62]. The reason could be that the opportune deformations that would otherwise exist in clean sand will be restricted by the occupation of some of the voids by fines, resulting in a diminished increase of the dynamic modulus over the static modulus [77]. Radhakrishnan and Rohani [77] also reported a similar trend, with a dynamic modulus ratio between 1.04 and 1.38 for load rise time ranging from 8 to 10 msec.

Table 1
Summary of HSR uniaxial compression tests on sand from the literature.

Reference	Loading mechanism	Peak applied stress	Sands tested	Saturation	Load rise time	Comments
Whitman [73]	Hydraulic/Gas driven piston	1.4 MPa	Fine sand	Dry and Saturated	15 ms	Multiple wave reflection theory first developed; Uniform stress distribution achieved
Heierli [66]	Drop weight, 50–160 kg, 1.8 m max. drop height	~1.7 MPa	Well graded sand; Well graded gravel	Partially saturated	~5 ms	Repeated loading considered; Wave propagation studied; Analytical theory developed based on experiments
Schindler [68]	Gas driven piston	2.07 MPa	Poorly graded fine sand	Dry	25 ms	Improved version of earlier devices used [73]
Schindler [69]	Gas driven/Explosive driven piston	2.07 MPa	Fine silty sand	Dry	5 ms	Improved loading setup used to reduce load rise time
Jackson et al. [72]	Gas driven/Explosive driven piston	40 MPa	20-40 Ottawa Sand; Poorly graded backfill sand	Dry	0.3 ms	Multiple reflection theory applied; Inertial forces affected results of tests with load rise time below 0.3 ms
Whitman et al. [26]	Hydraulic driven piston	690 kPa	Uniform sand	Dry	3 ms	Wave propagation considered; effect of stress level on wave propagation velocity studied
Farr [62]	Gas driven/Explosive driven	69 MPa	Poorly graded quartz and carbonate sands,	Partially saturated	0.4 ms	Careful sample preparation procedures were followed; Re-analysis of previously published data showed that tests at load rise times below 0.3 ms were unreliable
Akers [74]	Gas driven piston	95 MPa	Poorly graded calcite sand	Partially saturated	6 ms	Post dynamic loading creep tests were also reported; drained and undrained tests reported

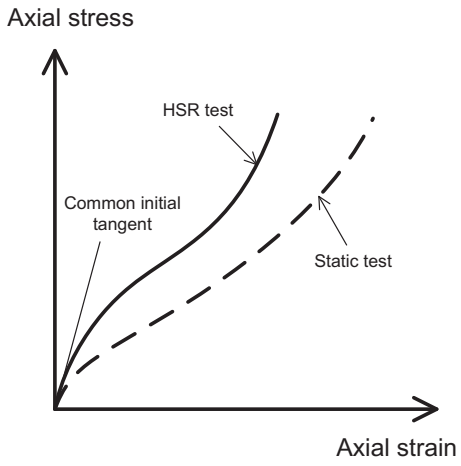

Fig. 6. Schematic representation of the effect of high strain rate on the stress-strain response of sand in uniaxial compression (redrawn per Whitman et al. [26]).

The stress in HSR uniaxial compression test can be normalized by the static stress from a conventional test, to illustrate the increase in stiffness due to HSR loading at different strains. Uniaxial compression tests by Farr and Woods [70] and Akers [74] have been normalized and summarized in Fig. 9, with the axial strain plotted in logarithmic scale to magnify the trends at small strains. The figure demonstrates that (1) the faster the rise time the higher the rate effect, although there may be a contribution of inertial effects as well at very small strains. (2) The increase in the normalized stress ratio is not constant over the first 2–4% strain, with the stress ratio inversely proportional to rise time. (3) The strain rate effect diminishes with strain up to approximately 4%. (4) The normalized stress ratio remains relatively constant as loading progresses beyond 2–4% strain. This suggests that the strain rate effect on the stress-strain response remains relatively constant over a wide range of strains beyond the small strain range of 0–4%.

4.3. *Effect of saturation*

The degree of saturation is an important contributing factor to the HSR uniaxial compression response of sand, although little supporting data is available. Intuitively one expects that under HSR loading of saturated sand there will be insufficient time for the dissipation of excess pore pressures, and the behavior would essentially be that of undrained sand. Fully saturated sand is very stiff, dominated by the highly incompressible pore water [21]. Pore air offers no resistance to HSR loading, compared to water, making the response of dry or unsaturated sand softer than that of saturated sand. The transition from soft to stiff response has not been studied in sand under uniaxial compression. However, the behavior can be gleaned from tests conducted by Farr [62,181] on Vicksburg loess. The response of partially saturated sand under HSR loading depends on the applied stress level, and the degree of saturation. The response of partially saturated sand is schematically represented in Fig. 10, depicting the two effects of increasing the degree of saturation on the response, i.e., softening of the initial response, and a stiffer response at higher strains with increasing degrees of saturation.

The effect of the degree of saturation on HSR uniaxial compression response of sand has been more extensively studied using SHPB, triaxial tests, and plate impact tests, and is discussed in the following sections.

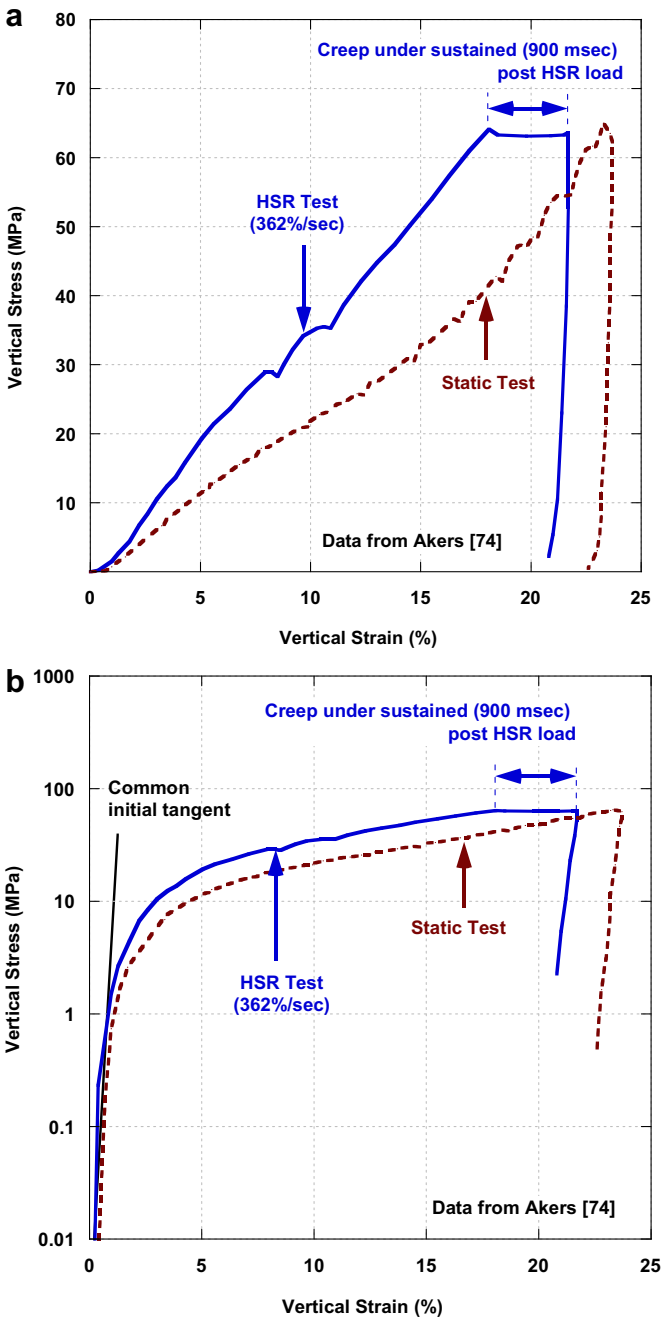

Fig. 7. Comparison of the stress-strain response of sand in uniaxial compression from static and HSR tests.

5. Split hopkinson pressure bar (SHPB) test

5.1. *Background*

The Split Hopkinson Pressure Bar (SHPB) was originally developed by Hopkinson [78] and was further developed to its present form by Kolsky [79], and is the most common experimental method used in the study of engineering materials under HSR loading [16]. Tests are performed by placing a specimen of the material to be tested in between two long bars that are hard enough to remain elastic, termed incident bar and transmitting bar. A third bar called the striker bar is propelled, typically using a gas gun, to strike the incident bar. The impact generates an elastic compressive wave in

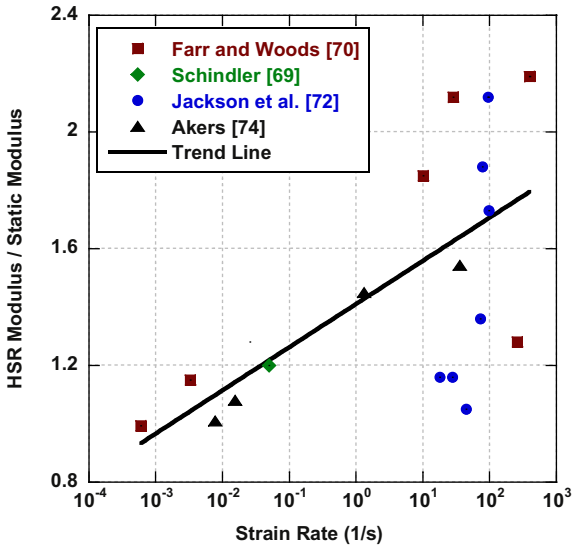

Fig. 8. Dynamic modulus ratio as a function of strain rate.

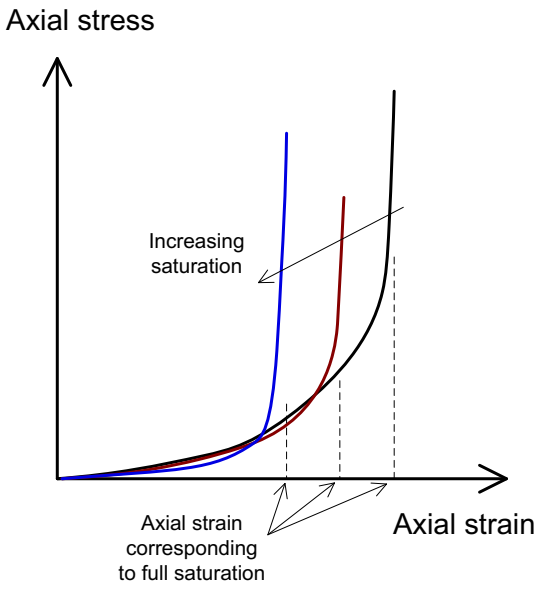

Fig. 10. Effect of the degree of saturation on uniaxial compression response of soils (Based on data by Hendron et al. [180]).

the incident bar which then travels through it and reaches the bar–specimen interface. At the interface, part of the wave transmits into the test specimen and through the transmitting bar, while part of it reflects back and travels into the incident bar. By placing strain gauges on the incident and transmitting bars, the reflected and transmitted waves are measured on the surface of the bars.

If a uniform stress distribution is assumed over the length of the specimen, then analysis of the strain in the incident and transmitting bars gives the engineering stress and strain in the sample. In order to account for inertial effects in the soil specimen a Lagrangian analysis has been used to correct the initial portion of the stress-strain response, usually comprising up to the first 100 μs [80,81]. Other corrections and modifications to the testing and measurement methods can be found in [17,82]. A summary of SHPB tests on sand is presented in Table 2.

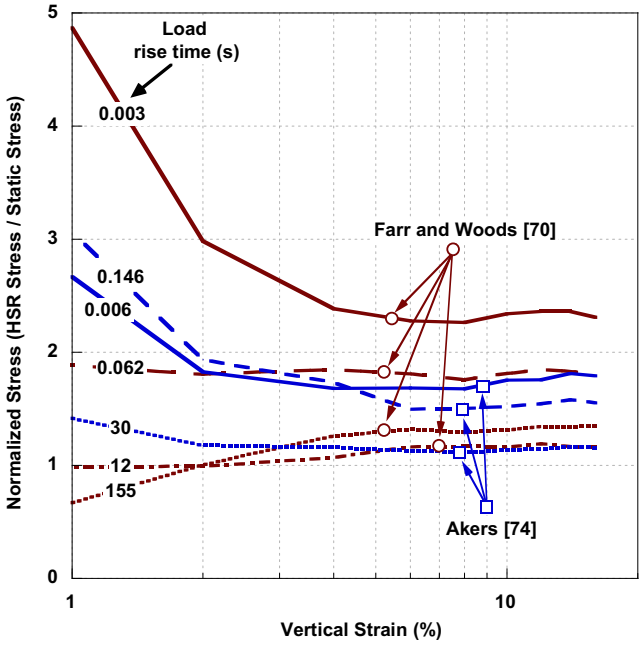

Fig. 9. Normalized stress at different strains in HSR uniaxial compression tests.

5.2. Stress uniformity in SHPB tests

The most important criterion for reliable results to be obtained from an SHPB test is to ensure that the stress distribution within the sample is uniform [83]. This implies that the stress gradients should have diminished due to multiple reflections of the propagating stress wave, as previously discussed for uniaxial compression tests.

An effective method for achieving stress equilibrium in a soil specimen in SHPB tests is to modify the applied stress wave to increase the rise time, allowing multiple reflections to occur within the specimen by the time the applied stress reaches its maximum value. This can be achieved by employing pulse shaping techniques [84,85], which involves placing a thin plate or disk, usually made of steel or copper, on the striker end of the incident bar. An analogy to pulse shaping in geotechnical engineering is the use of cushions in pile driving. Song et al. [86] and Luo et al. [88] have recently reported the successful employment of pulse shaping techniques to achieve uniform stress distribution in SHPB tests on dry sand. The stress time histories of several reported SHPB tests on sand are shown Fig. 11. It can be seen that comparing to the earlier tests performed by Felice et al. [87] the use of pulse shaping techniques significantly lengthens load rise time, thus ensuring stress equilibrium is reached during the constant strain rate portion of the test.

It is important to monitor the strain and strain rate time histories in an SHPB test in order to ascertain the extent to which a constant strain rate (CSR) condition exists during the test. If the goal is to explicitly derive strength or modulus as a function of strain rate, then observations of the HSR response will only be valid for the CSR portion of an SHPB test. Fig. 12 shows several such curves derived from the literature illustrating the extent to which it has been feasible to achieve CSR conditions in an SHPB test on sand. For example, it can be seen that Luo et al. [88] were able to achieve a near CSR of 600/s for approximately 150 μs of loading, corresponding to strains up to nearly 10% in the sample. It is also evident from Fig. 12 that although it is possible to increase the strain rate, it is not necessarily ensured that a CSR condition is sustained in the test. Moreover, it can be seen that samples experience a large strain prior to reaching the CSR state. Interpretation of results therefore

Table 2
Summary of SHPB tests on sand from the literature.

Reference	Peak pressure	Soils tested	Saturation	Max. strain rate	Comments
Fletcher and Poorooshasb [164]	~0.84 MPa	Fine grained soils	Partially saturated	200/s	One of the first SHPB studies on soils reported; inertial effects not clearly considered
Gaffney and Brown [165]; Gaffney et al. [166]	500 MPa	Clayey silty sand	Partially saturated	5000/s	Negligible strain rate effects observed
Felice [83] and Felice et al. [87]	760 MPa	Clayey silty sand	Dry/Partially saturated	5000/s	Effect of saturation studied
Ross et al. [167]	10.3 MPa	20/40 and 50/80 silica sand	Dry/Partially saturated	NA	Long samples up to 15 cm tested; Wave propagation speed measured
Pierce [94]; Pierce and Charlie [95]; Charlie at al. [107]	4.5 MPa	50/80 silica sand; 20/30 Ottawa sand	Dry, partially and fully saturated	NA	Wave propagation speed studied; effect of saturation considered
Veyera [168]	225 MPa	Eglin, Tyndall and Ottawa 20-30 sand	Partially saturated	2000/s	Effect of saturation studied
Semblat et al. [93,169]	750 MPa	Fine sand	Dry	1245/s	Lateral stresses measured; Effect of lateral confinement studied
Bragov et al. [91]	500 MPa	Fine quartz sand	Dry	NA	Lateral stresses measured; Plate load tests reported as well
Bragov et al. [91,92]	400 MPa	Fine sand	Dry	NA	Wave speed propagation studied; numerical model applied; lateral stress
Martin [96] Martin et al. [106]; Martin and Chen [170]	~35 MPa	Poorly graded fine quartz	Dry/Partially saturated	470/s	Effect of saturation studied; pulse shaping techniques used
Song et al. [86]	~31 MPa	Fine silica sand	Dry	1450/s	Effect of lateral confining studied by using different confining tubes
Luo et al. [88]; Lu et al. [89]	360 MPa	Fine quartz sand	Dry	680/s	Sample preparation and relative density carefully controlled; lateral stresses recorded
Kabir [171]; Kabir et al. [98]	150 MPa	Fine silica sand	Dry	470/s	Triaxial SHPB tests performed; Pulse shaping techniques used

requires careful consideration of the effect of the changing strain rate at the early stages of testing.

5.3. Effect of lateral confinement

SHPB tests on sand are commonly performed by placing the sample within hardened steel confining cylinder; ideally this provides a rigid boundary and the load path is uniaxial strain. Employing a softer material for confinement will allow higher radial strains as the impact axial load is applied, and the response will deviate from a lock up behavior (zone 3 in Fig. 1) to shear hardening response with a sustained maximum shear stress. If an adequately soft confinement is employed, the sample will sustain a limiting stress which may be used to define shear strength [86,89–92] under HSR loading. The effect of confinement is illustrated in Fig. 13a, where specimens of sand were confined in cylinders having different properties. It can be seen that specimens confined in rigid cylinders sustain a higher stress. As the level of confinement decreases the soil can sustain less axial stress. Numerical analysis performed by Goh et al. [36] suggest a similar trend (Fig. 13b), indicating that as the lateral confinement decreases the mean stress path tends to move closer to the critical state line (CSL), and eventually reaches the CSL at some limiting lateral confinement, indicating a shear failure. Similar trends have also been reported by Semblat et al. [93]. It is further deduced from Fig. 13b that the fully confined soil sample does not reach the CSL, and that shear failure as defined in critical state soil mechanics does not occur under uniaxial compression. It is important to note, however, that when samples are allowed to deform laterally, extra lateral confinement due inertial effects contribute to the HSR response, and should be taken into account in interpretation of results. Erroneous interpretations of SHPB tests as a result of neglecting these inertial effects have been widely reported in the literature for other geomaterials such as concrete, as discussed by Li and Meng [60] and Lu and Li [100].

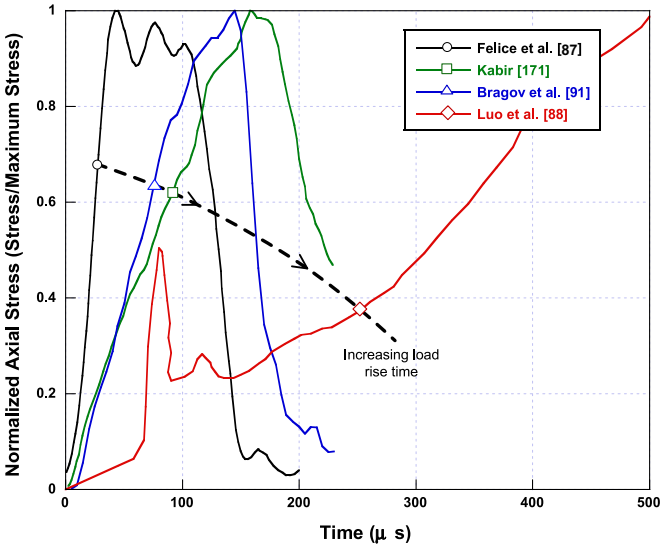

Fig. 11. Effect of pulse shaping techniques on the stress history of specimens of sand in SHPB tests.

Measurement of lateral stresses and strains allows for constitutive laws to be established for HSR behavior of sand based on SHPB tests. SHPB setups have been recently modified to allow for controlling the lateral stress during testing. Pierce [94] and Pierce and Charlie [95] innovated the use of confining pressure in the SHPB test by placing the sample in a deformable membrane and applying a confining pressure using a thin layer of pressurized water between the membrane and the confining cylinder. Martin [96], Kabir and Chen [97] and Kabir et al. [98] have recently reported successful triaxial SHPB tests on sand with confining pressures of up to 150 MPa. In these tests confining pressure is applied by means of two pressure chambers; a radial confining pressure chamber encasing the sample,

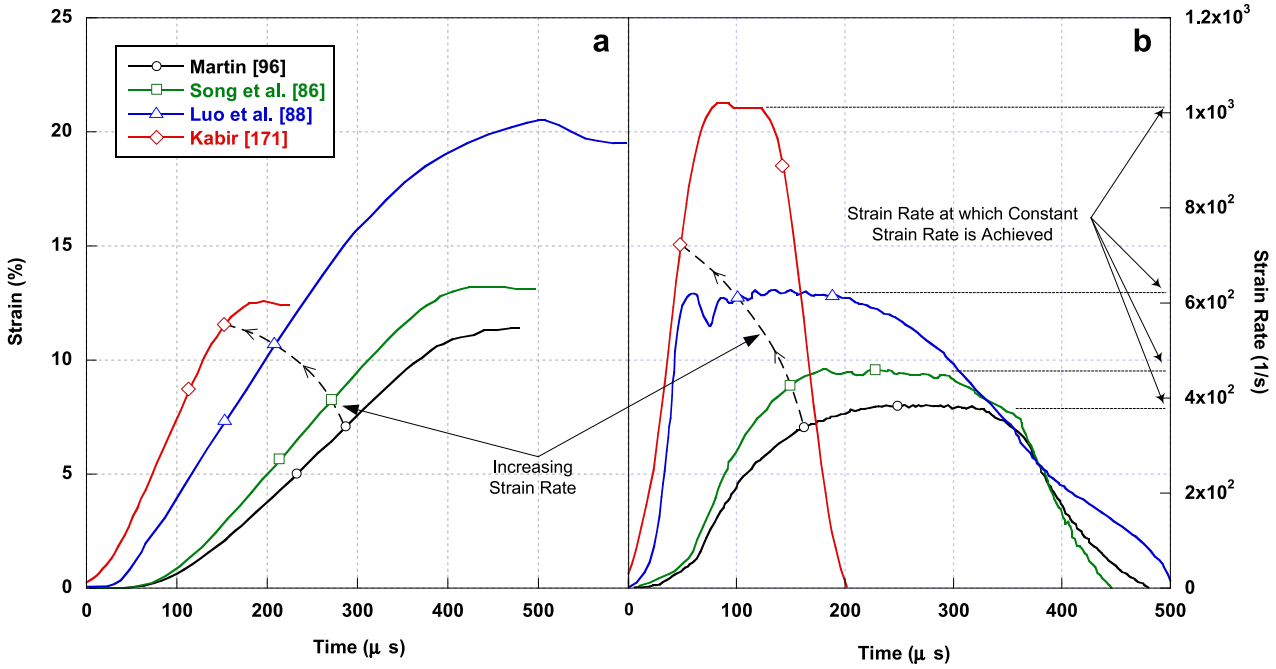

Fig. 12. Strain and strain rate time histories of SHPB tests on sand a) strain time history; b) Strain rate time history.

and an axial confining chamber at the opposite end of the transmission bar. The two chambers apply equal pressures to the sample in the axial and radial directions to produce hydrostatic confinement. Dynamic deviatoric stress is then applied by means of the striker bar. The effect of confinement on HSR stress-strain response is shown in Fig. 14. Similar to static loading, confinement results in a stiffer soil response, due to the increase in frictional resistance of sand as a result of increase in ambient stress. Moreover, the stress-strain curves over a wide range of high confining pressures indicate that the specimens regain strength following an initial yield at lower strains. It is important to note that the triaxial SHPB tests reported by Kabir et al. [98] were performed at high confining pressures of up to 150 MPa, where grain crushing during the consolidation phase has been reported to dominate the response in shear [48,99]. Finally, triaxial SHPB tests suggest that increasing the strain rate from 500/s up to 1000/s has negligible effect on the stress-strain response of sand. As will be discussed in next sections, some of these observations are in contrast with the observations from conventional triaxial tests performed on sand.

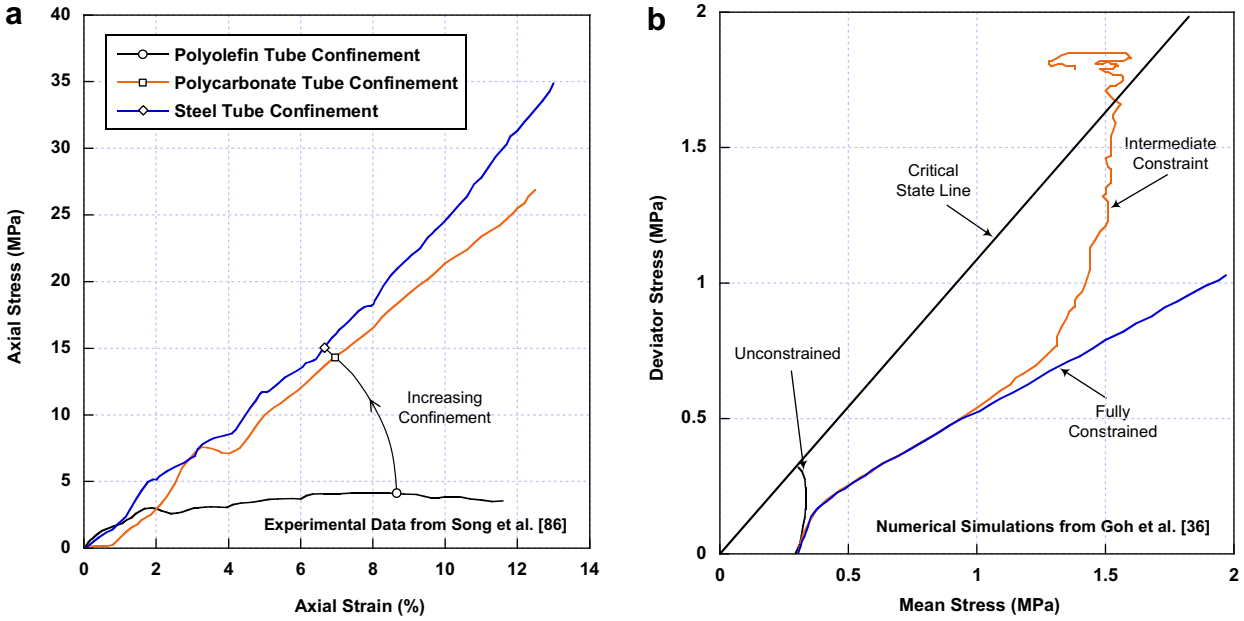

Fig. 13. Effect of lateral confinement on stress-strain response of a) Sand from SHPB tests (Scatter not shown); b) Numerical simulation of mean stress path from uniaxial compression tests with various lateral confinements.

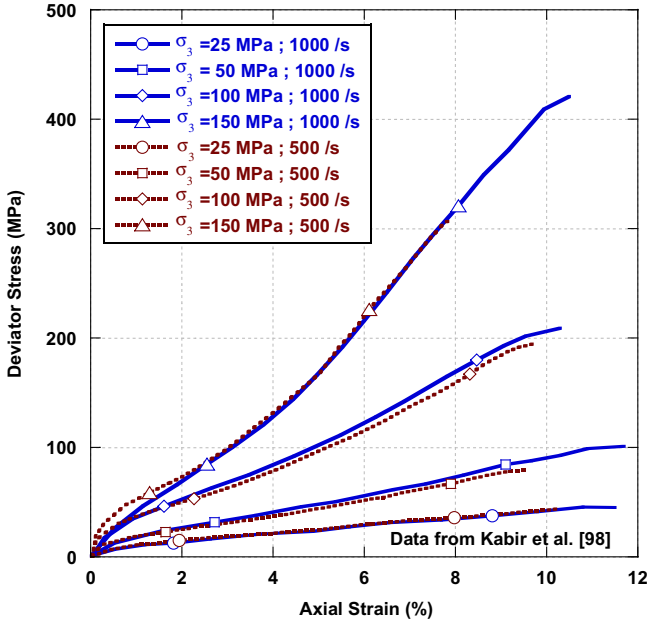

Fig. 14. Effect of confining pressure on HSR stress-strain response of dry sand from triaxial HPB tests (note: 1/s = 100%/s).

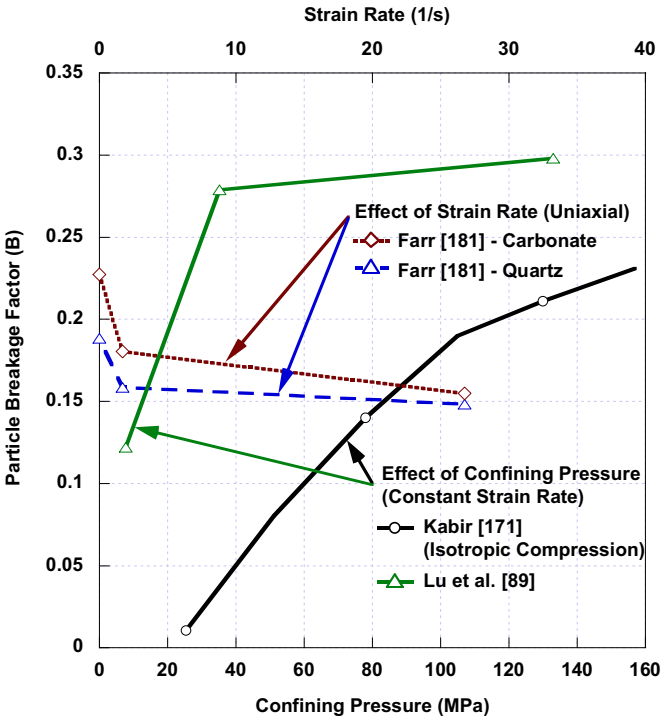

Fig. 15. Effect of confining pressure and strain rate on particle breakage factor in uniaxial compression and triaxial SHPB tests (approximate strain rate calculated from uniaxial tests based on time to peak stress).

5.4. Grain fracture

Study of particle breakage has been facilitated by recently reported triaxial SHPB tests. Although comprehensive systematic studies are yet to be performed, grain size distribution curves from the limited data available may be employed to quantify particle breakage. The particle breakage factor, B, has been used with different definitions by several authors including Marsal [101], Lee and Farhoomand [102], Hardin [103], Lade et al. [104] and Nakata et al. [105]. The general definition given by Hardin [103] has been adopted here, where B is defined as:

$$B = \frac{B_t}{B_p} \tag{1}$$

where B_p is the breakage potential defined as the area between the original grain size distribution curve of the soil limited in the lower bound by the No. 200 sieve (0.074 mm sieve opening). B_t is the total breakage potential defined as the area between the original grain size distribution curve and the final grain size distribution curve.

The effect of confining pressure on particle breakage in HSR tests on sand has been depicted in Fig. 15 from triaxial SHPB test data presented by Kabir et al. [98]. It can be seen that similar to the case of static loading, particle breakage in shear increases with increasing confining pressure under HSR loading. However these tests may be affected by grain crushing during the consolidation stage. Static triaxial test results reported by Murphy [48,99] suggest that grain mineralogy is a significant factor in shear resistance under high confining pressures. Accordingly, with softer grains, crushing contributes to shearing resistance under lower confining pressures. However, at high confining pressures (in the range of 300 MPa from tests reported by Murphy [48]), grain crushing has negligible contribution to shearing resistance, as significant grain crushing has already occurred in the consolidation stage. In harder grained soils, crushing and degradation of grains continues to contribute to shearing resistance under high confining pressures.

The effect of strain rate on B is also shown in Fig. 15 using data reported by Kabir et al. [98] using recently developed triaxial SHPB tests where confining pressure is controlled, and Farr and Woods [70] data obtained in HSR uniaxial compression tests. Tests by Farr and Woods are stress-controlled, in which load rise time was reported in the original publication, and approximate strain rates have been calculated in Fig. 15 based on sample size. It is evident that the rate of particle breakage at a given initial void ratio decreases slightly as the strain rate increases, in both tests, due to the time-consuming nature of particle crushing. Although the B factor indicates that the magnitude of grain crushing is affected by HSR loading, it does identify the nature of crushing. Grain crushing in shear of angular sand results in breakage of the asperities, producing grains of relatively comparable size to the original grains, along with high quantity of fines. The definition of the B factor should therefore be extended to include fines produced as a result of crushing, as suggested by Sadrekarimi and Olson [52]. It is comparably important to note that the time-dependent nature of particle breakage also depends on particle shape and size, factors which have not yet been explicitly addressed under HSR loading.

Finally, it is noted that the B factors calculated in Fig. 15 employ different values of the lower grain size limit to derive B_p, due to unavailability of data in some cases. The values plotted are therefore intended for qualitative representation of the crushing phenomenon, and should not be used in quantitative comparison of breakage potential of the soils under discussion.

5.5. Effect of saturation

The stress-strain response of partially saturated sand depends on the confining pressure, initial void ratio and the degree of saturation. The role of partial saturation in stress-strain response of sand under static loading is related to capillary forces. Depending on the structure of the porosity at the mesoscale, these capillary forces may increase apparent cohesion, thereby increasing resistance to shear deformation. Under HSR loading the response may be dominated by air or water depending on the

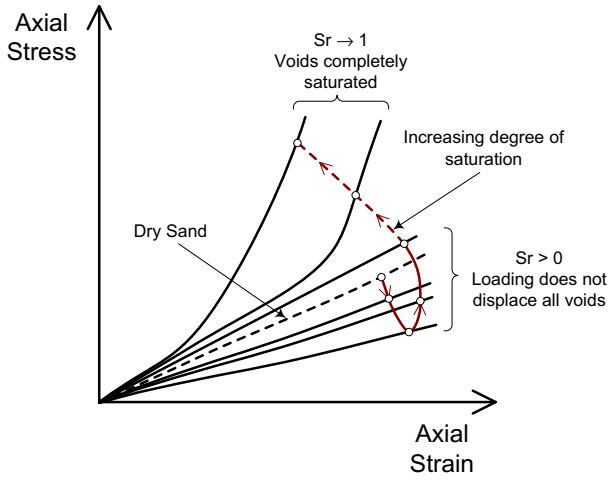

Fig. 16. Two limiting conditions in conventional SHPB tests on partially saturated sand.

degree of saturation. Water is much stiffer than air. If the strains produced by the HSR loading are not sufficient to displace all the air voids, the stress-strain response will not exhibit a lock-up response, as indicated in Fig. 16 and supported by data from the literature shown in Fig. 17. Under such loading conditions partially saturated sand is more compliant compared to dry sand and the stiffness degrades with increasing saturation, up to the saturation degree associated with air void closure. At high saturation degrees the voids may become saturated under HSR loading and the response will be essentially governed by the water in the pores as shown in Fig. 17b.

The initial softening response at lower saturation degrees is due to two possible explanations as discussed by Martin et al. [106]. First, the addition of water acts to lubricate the sand particles thus reducing friction and offering less resistance to compression. Introducing more water will further ease compression, up to a point where the air within voids is nearly fully displaced by water, making it difficult for sand particles to displace into the interstitial gaps. From this point on, increasing the degree of saturation gradually increases stiffness. The initial response is due to lessened shear resistance due to reduction of contact stresses, while the later response results from elimination of free volume. Second, water added to a dry sand specimen acts as lubricant along the soil-confining cylinder interface and the end platens, allowing the specimen to compress with reduced resistance offered by the boundaries. While the former explanation represents effects of saturation on intrinsic soil properties, the latter is merely due to testing boundary conditions and does not represent field behavior. The assumption that water has a lubricating effect on sand is not universal: Horn and Deere [33] observed that adding water to rough surfaced dry Ottawa sand has little effect on shearing resistance aside from the capillary forces generated. It has even been shown that water acts as an anti-lubricant on smooth surfaced minerals. Elucidating the effects of saturation on HSR response of sand therefore requires closer examination of mineral structure and surface texture of grains. It is noteworthy that under high axial stress, the air voids in partially saturated sand may be entrapped and dissolved in the pore water, resulting in partially saturated sand behaving as if it were fully saturated. The strain required to reach this *quasi-saturated* state depends on the initial degree of saturation as shown in Fig. 16. An increase in the quasi-static modulus of partially saturated sand reported by Charlie et al. [107] may be explained based on the above discussion.

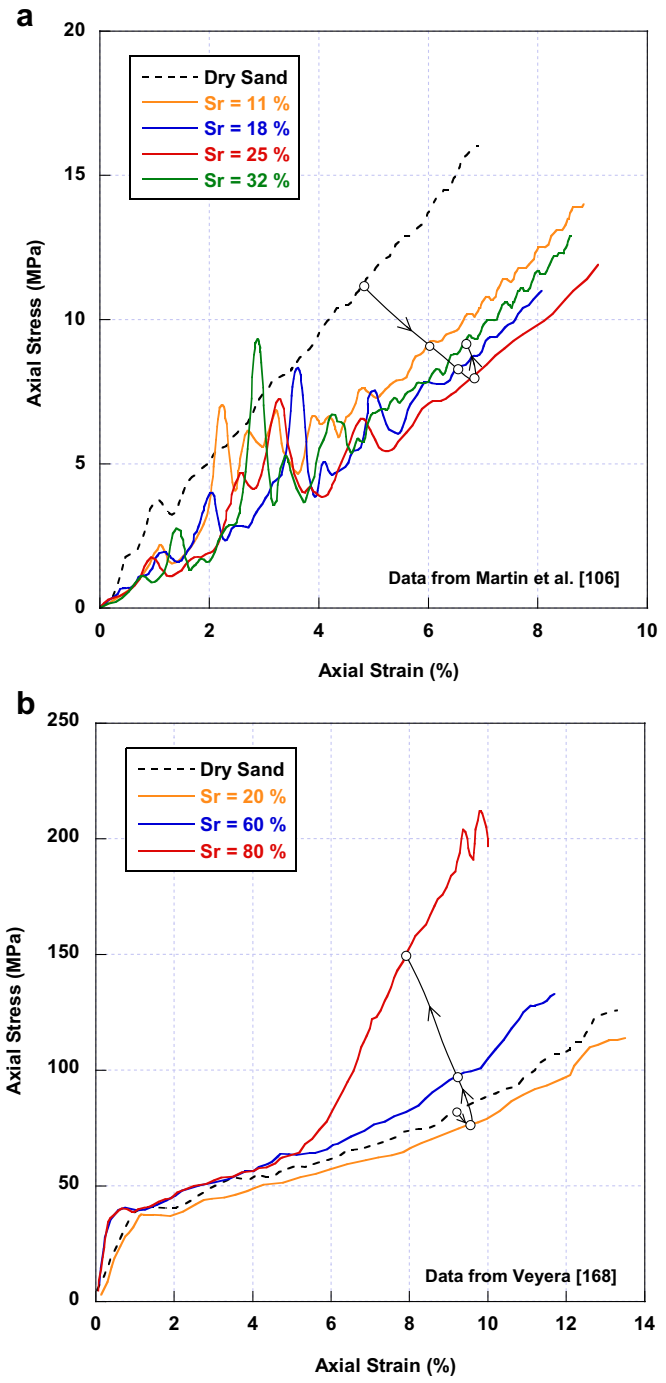

Fig. 17. Effect of saturation on HSR response of sand in SHPB tests; a) Softening of response as saturation degree increases, with no lock up observed, b) Lock up behavior observed at high saturation degrees.

Finally, although SHPB tests on fully saturated sand with measurements of pore pressure are not available in the literature, recent shock loading tests (uniaxial compression) reported by Veyera et al. [108] suggest that considerable residual pore pressures may be produced at low axial strains in fully saturated sand under HSR axial loading. Measurement of residual pore pressures is important due to the potential for liquefaction if the pore pressure ratio, defined as the ratio of pore pressure to total stress, approaches a unit value. Veyera et al. [108] observed that both loose and dense sand liquefied under the application of several low

amplitude shock loadings, apparently due to grain crushing. Liquefaction due to HSR loading has been observed earlier by other authors as well [109]. Thompson [110], for example, reported partial liquefaction of loose saturated sand when subject to projectile penetration that is dominated by HSR loading. Savvateev et al. [111] also reported a decrease in resistance to projectile penetration of saturated sand compared to dry sand. However, the earlier studies suffer from limitations in pore pressure measurement methods for HSR loading. Experimental investigations using more recent developments in instrumentation methods seem necessary in order to elaborate further on the relationship between HSR loading of sand and the liquefaction phenomenon.

5.6. Strain-Rate effects

Contrary to other geomaterials such as concrete, SHPB tests on dry sand have generally indicated little strain-rate dependency in terms of the stress-strain response. Semblat et al. [93], Song et al. [86] and Kabir et al. [98] have all reported insignificant strain-rate effects for stress magnitudes up to 200 MPa and strain rates exceeding 1000/s. Despite these observations, post test analysis of particle gradation (Fig. 15) indicates that particle breakage decreases by increasing the strain rate, suggesting that particle crushing is time consuming, and that the mechanisms involved in particle crushing under uniaxial loading are affected by HSR loading. Insensitivity of the stress-strain response to this particle crushing may be due to several factors, including: (1) smaller crushed particles may interact similar to the larger grains; (2) larger particle size may be necessary in order to observe crushing effects, but the sands used in SHPB tests tend to be very fine grained; (3) test boundary conditions may be affecting the mechanical response in SHPB tests. One such effect stems from the small thickness of SHPB test specimens. In triaxial SHPB tests, for example, a small sample thickness may prohibit the formation of shear bands. Analysis of the HSR response at the mesoscale is thus required in order to better understand the effects of HSR on the behavior of sand.Very limited available data suggest that partially saturated sand exhibits strain-rate dependency to some extent. Felice [83] noticed that specimens with water content near the optimum moisture content (moisture content required for achieving maximum dry density in laboratory compaction tests) exhibit strain-rate sensitivity at strains larger than that required for the water to dominate the response. He concluded that pore water pressures play an important role in the observed strain-rate response. These limited observations may have been the result of boundary effects, and, since little work has been done to study these effects in unsaturated soils, it is difficult to draw any definite conclusions on the strain-rate dependency of partially saturated sand, and there is a clear need for further research in this area.

6. HSR triaxial shear test

6.1. General comments

Extension of conventional triaxial tests to monotonic HSR loading requires modification of the axial loading apparatus to allow for application of impact-type loads. The most common systems used to generate HSR axial loading in triaxial shear device may be divided into two main categories: (1) drop weight systems and (2) pneumatic and hydraulic pistons (Table 3).

It has generally been established that under rapid loading conditions saturated triaxial test specimens approach undrained conditions. Seed and Lundgren [112] noticed that under rapid transient loads even in drained tests on coarse sand there is not enough time for drainage to occur and test conditions are actually undrained. Attempts to measure pore pressures in undrained impact tests have been reported in the literature, including Whitman and Healy [109,113] who inserted a needle at mid-height of the specimen and used a pressure transducer to measure pore water pressures. However, pore pressure distribution is expected to be non-uniform during a rapid test, and measurements of pore pressures during undrained impact tests are scarce.

At very high strain rates, even the pore air in dry sand will experience a small increase in pore air pressure, which can be significant at low confining pressures [114]. Vacuum triaxial tests may be performed in such cases to eliminate the buildup of pore pressures in dry drained HSR tests on sand. In addition to eliminating pore air pressure buildup, subjecting the sample to vacuum produces the effect of confinement as well.

6.2. Sample size and inertial effects

Application of HSR load to a triaxial soil sample generates axial and radial inertial forces as the sample accelerates at its boundaries. The inertial forces appear in the axial direction in the form of increased resistance to the applied load, and in the form of increased confinement in the lateral direction, as depicted in Fig. 18. The magnitude of inertial forces depends on size and mass of the soil sample being tested, and is higher near the moving boundaries. Whitman and Healy [109,113], suggested that inertial effects will be

Table 3
Summary of HSR triaxial tests on sand from the literature.

Reference	Loading mechanism	Saturation	Confining pressure	Test method	Maximum rate of loading
Casagrande and Shannon [172,173]	Dropweight	Dry and Saturated	30–90 kPa	Drained Triaxial Compression	0.2 m/s
Seed and Lundgren [112]	Dropweight	Saturated	197 kPa	Drained and Undrained Triaxial Compression	1.02 m/s
Taylor and Whitman [174]	Hydraulic	Saturated	100 kPa	Vacuum Triaxial and Undrained Triaxial Compression	0.005 s load rise time
Whitman [117]	Hydraulic	Dry, Moist, and Saturated	100–414 kPa	Drained and Undrained Triaxial Compression	11/s
Whitman and Healy [109]	Hydraulic	Dry and Saturated	70 kPa	Vacuum Triaxial Compression	0.5 m/s
Saxe et al. [175,176]; Schimming et al. [116,177]	Pneumatic and Hydraulic	Dry	–	Direct Shear	5 ms load rise time
Lee et al. [43]	Pneumatic	Saturated	101–1472 kPa	Undrained Triaxial	0.22 m/s (2.50/s)
Carroll [178,179]	Hydraulic and Pneumatic	Dry and Moist	345–1379 kPa	Undrained Triaxial Compression	2 ms to failure
Abrantes [125], Abrantes and Yamamuro [122,123], Yamamuro and Abrantes [135]	Dropweight	Dry	98–350 kPa	Vacuum drained triaxial Compression	17.50/s (Load rise time $<$ 5 ms)
Huy et al. [114]	Hydraulic	Dry and saturated	100 kPa	Undrained	4.20/s

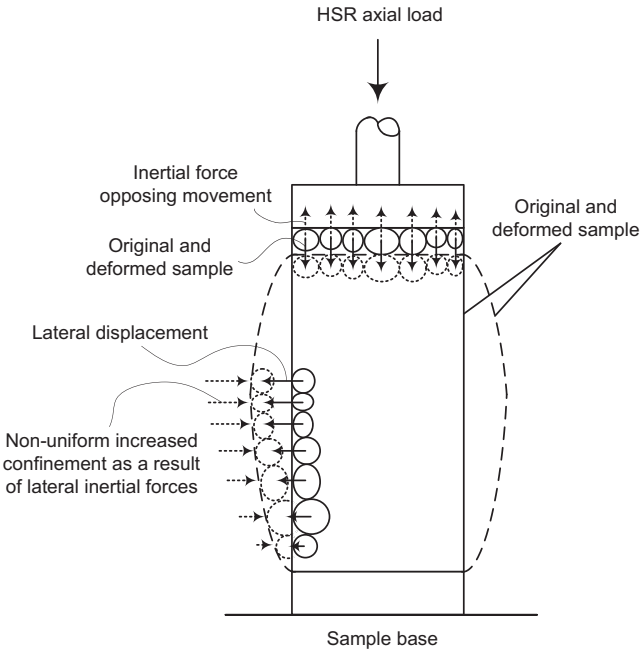

Fig. 18. Axial and lateral inertial effects in an HSR triaxial test specimen.

minimal if the load rise time is limited so that the propagating stress wave is allowed to travel back and forth at least ten times within the sample before the peak of the HSR stress is reached. Inertial effects may also be attributed to test boundary conditions such as the loading mechanisms and the confining system. These inertial forces are not attributed to intrinsic soil properties, and should therefore be minimized.

An interesting study of inertial effects due to boundary conditions on mechanical response of sand was reported by Schimming and Saxe [115] and Schimming et al. [116]. They employed direct shear tests in which the confined sand to be tested was placed between two platens with a normal force applied, and HSR shear displacements were imposed on one platen while the other was fixed. Two sets of HSR tests were performed in which all parameters were similar except for the method of applying the normal stress. In the first set of tests, the normal stress was applied by using dead weights, while in the second set of tests a pneumatic system was employed to apply the same magnitude of normal stress. The static tests and the HSR tests using pneumatic normal stress yielded similar failure envelopes with a friction angle of 43°, whereas the HSR tests using mass system normal stress gave a jump in friction angle to 61°. Since all tests were performed under identical normal stress magnitudes, the difference in the two sets of HSR tests were attributed to inertial effects in the loading mechanisms. Accordingly, as the HSR load is applied, the soil tends to shear along the shear surface by dilating, but inertial forces prevent upward movement of the top half of the shear box. Therefore, shearing of the soil becomes possible only by shearing of the grains, resulting in higher shearing resistance.

6.3. Shear strength under HSR loading

HSR behavior of sand may be elucidated by referring to the controlling mechanisms in shear under quasi-static loading. HSR loading effects may be discussed in terms of the contributing components of shear resistance: inter-particle friction, geometric interference, and grain crushing. Limited studies suggest that inter-particle friction is not significantly affected by rate of shearing. Horne and Deere [33], found no distinguishable change in the inter-particle friction of quartz when sheared at rates in the range of 1.8–15.2 cm/s. HSR tests on sand have shown that under low confining pressures as the strain rate increases, the friction angle in both loose and dense sand first decreases slightly and then increases by up to two degrees beyond the static friction angle [21,114,117–121]. The initial decrease in friction angle has been attributed to kinetic friction acting between soil grains as opposed to the higher static friction [33]. The subsequent increase in the friction angle which corresponds to an increase in strength of up to 10% is evidently related to dilation in sand. As suggested in Fig. 19 and supported by recent studies [122,123], as strain rates increase under low confining pressures the tendency for dilation increases in sand and a transition from contractive behavior to dilative behavior is observed. Torsional shear tests by Healy [124] also suggested an increase in volume expansion of sand by 10%–15% at high strain rates. From a mesoscale point of view Abrantes [125] suggested that as the strain rate increases there is less opportunity for sand grains to find the easiest path past one another to fill the voids, and a change in particle trajectory occurs, as illustrated in Fig. 20.

The initial void ratio also contributes to the HSR response of sand. Dense sand exhibits a greater tendency for volume expansion under low confining pressures compared to loose sand. Therefore, HSR loading will have a greater influence on shear strength of dense sand, as illustrated in Fig. 19b. A summary of HSR triaxial test results from the literature is shown in Fig. 21 for both loose and dense sand where the peak strength from HSR tests is normalized by the peak strength from a static test. Strength is measured at peak deviatoric stress for dense samples (generally 2–4%) and at 15% strain for loose and medium dense specimens if a peak is not observed. At low to medium confinement both dense and loose sand exhibit marginal increase in strength at HSR below approximately 2/s. Above 2/s the strength increases by up to 30% in HSR loading relative to static loading.

Dense sand under very high confining pressure exhibits a stress proportional to log strain rate (Fig. 21). Under lower confining pressures sand exhibits a limiting strain rate behavior (Fig. 21). The trend observed for sand suggests that a remarkable change in the flow mechanics occurs under HSR loading which is controlled by the confining pressure. However, the aforementioned observations at high confining pressure are based on very limited data from Lee et al. [43] and there is very little supporting data available to draw definitive conclusions.

It may be postulated that HSR loading prevents grains from developing the geometric interference that is allowed in quasi-static loading through the time-consuming rearrangement mechanism of grains. Recent experimental and numerical studies on penetration of rigid projectiles in sand support this postulation through the observation that force chains develop differently under quasi-static and dynamic penetration of sand [126–129]. Under HSR loading, grains are forced to push and roll as opposed to quasi-static loading where grains rearrange to facilitate shear. Under HSR loading of dense sand at high confining pressures rolling and the associated volume expansion is restricted. Pushing of grains therefore accumulates strain energy up to the point of fracture. Under HSR loading, there is not enough time for strain energy accumulation [43,132], which prohibits crushing and promotes rolling-rearrangement resulting in a higher resistance to shear. The increased shearing resistance is also apparent from HSR triaxial data on medium dense and dense sand at low to high confining pressures, shown in Fig. 23, in which the deviator stress in each curve has been normalized by the maximum static deviator stress. It can be seen that the increase in strength due to HSR loading is

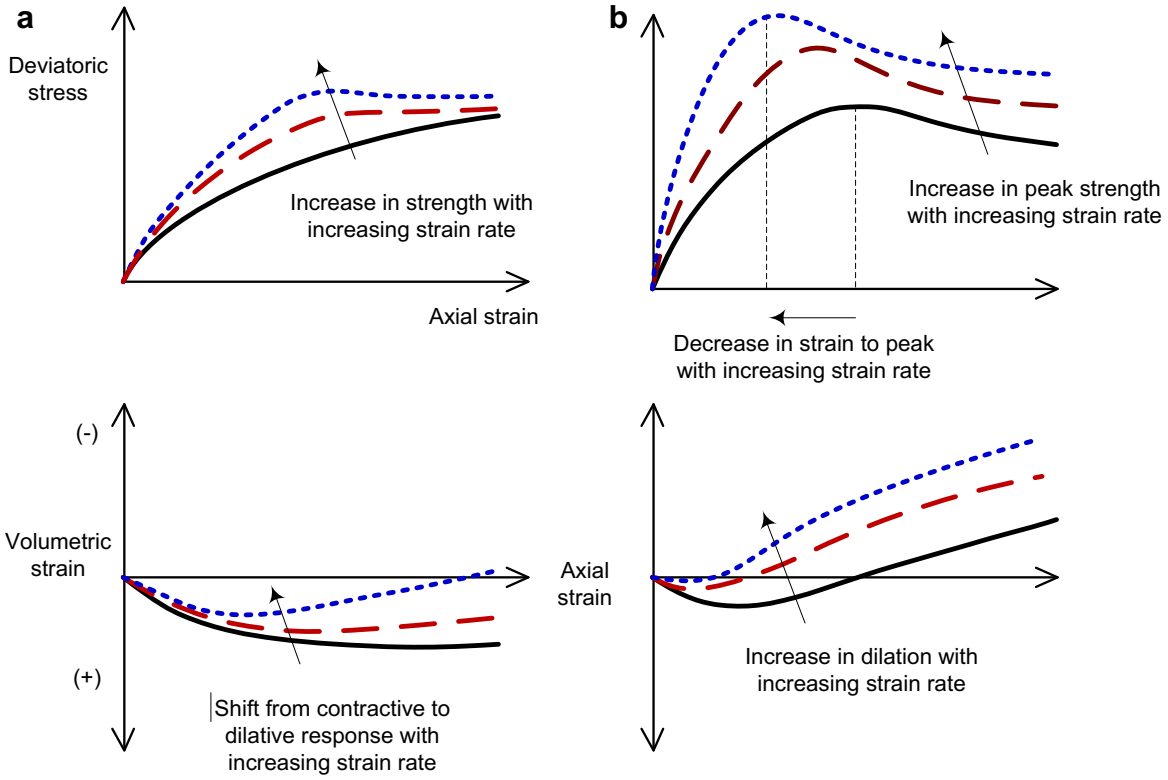

Fig. 19. Effect of increase in strain rate on stress-strain response and volumetric strains in (a) loose sand, (b) dense sand (interpreted based on data from Table 3).

greater at higher confining pressures. Evidently, raising the load strain rate up to only 0.5/s (50%/s) results in a nearly 30% increase in shear strength, indicating the significant effect of confining pressure on the HSR response of sand.

Dilation may also be studied through the dilatancy rate (d), commonly expressed as the ratio of volume change ($d\varepsilon_v$) to change in major principal strain ($d\varepsilon_1$), as follows [130]:

$$d = -\frac{d\varepsilon_v}{d\varepsilon_1} \tag{2}$$

The maximum dilatancy rate, d_{max} has been used by several authors in characterizing dilation of sand [131]. Study of data presented by Abrantes [125] and Yamamuro et al. [138] suggests that the rate of dilation is affected by HSR loading. It can be seen from Fig. 22 that HSR loading increases the dilatancy rate at failure in medium sand, but decreases the dilatancy rate at failure in loose sand. Furthermore, Fig. 22 suggests that increasing the confining pressure apparently magnifies the increase in dilation rate at failure. The increase in rate of dilation may be attributed to the decrease in grain fracture in two ways: (1) as grain fracture is prohibited under HSR loading shear may be accommodated only through further rolling and rearrangement of grains [43,136], and (2) Reduction in grain fracture decreases the associated local contraction, thereby magnifying the role of dilation in the global response.Indications of the latter mechanism have been observed in quasi-static loading as well [42]. Considering the importance of the aforementioned discussion, further research is required in order to understand the effects particle crushing, particle size, shape and mineralogy on HSR response of sand at various confining pressures. Results of such studies may eventually lead to incorporating rate effects in the components of friction suggested by Rowe [39] shown in Fig. 4.

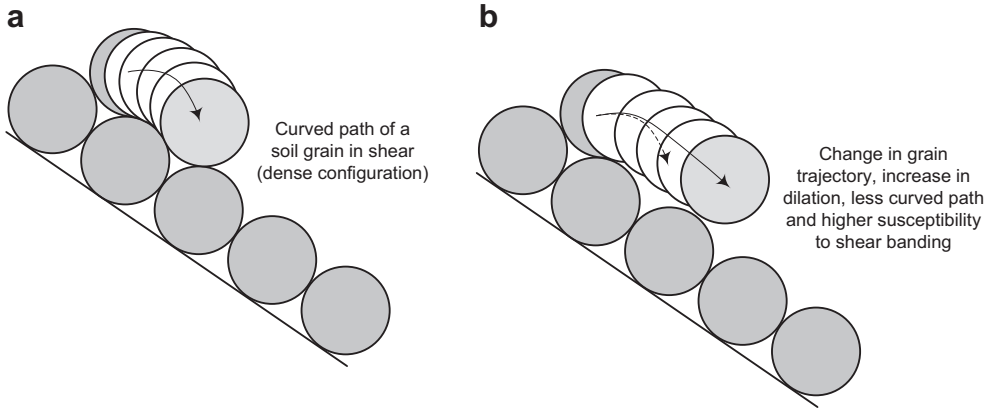

Fig. 20. Effect of HSR loading on sand particle behavior (modified from Abrantes [125]); (a) Static loading, (b) HSR loading.

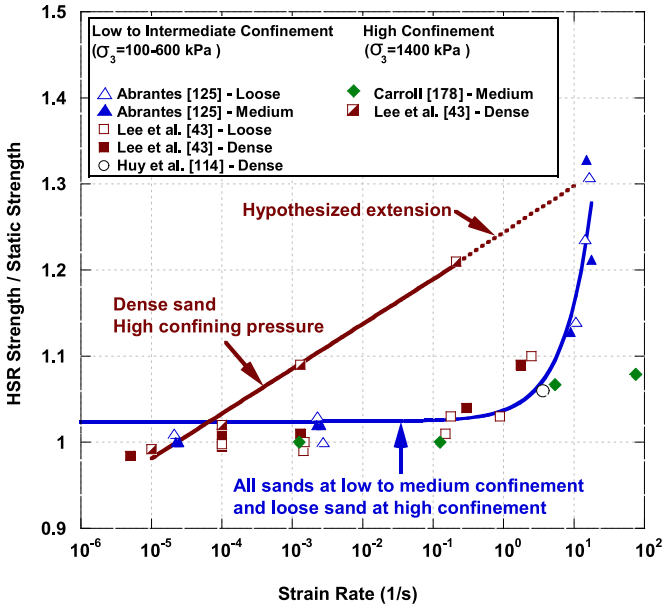

Fig. 21. Effect of HSR loading on shear strength of dry sand from triaxial tests.

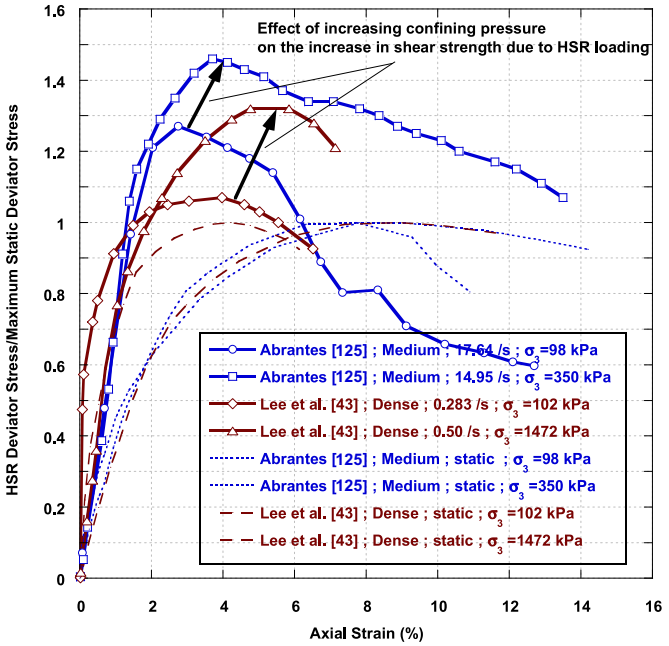

Fig. 23. Effect of confining pressure on normalized shear strength of dry sand under HSR loading.

6.4. Effect of saturation

The strength of saturated sand under HSR loading is influenced by volume change tendency in shear. Under static or slow loading loose sand tends to compress while dense sand tends to dilate. In undrained saturated sand dilation results in a decrease in pore water pressure and an increase in the effective stress (defined as the total stress minus the pore pressure), while contraction increases pore water pressure and reduces effective stress. Under HSR loading, Whitman [21] reported that an increase in strength of up to 200% can occur in loose saturated sand at low to moderate confining pressures. This large increase in strength results from the decrease in pore pressures as a consequence of tendency for dilation in the sample. It is noteworthy that the increase in tendency for dilation and the associated decrease in pore pressure serve to mitigate liquefaction potential in loose sand, as pointed out by Yamamuro and Lade [133].

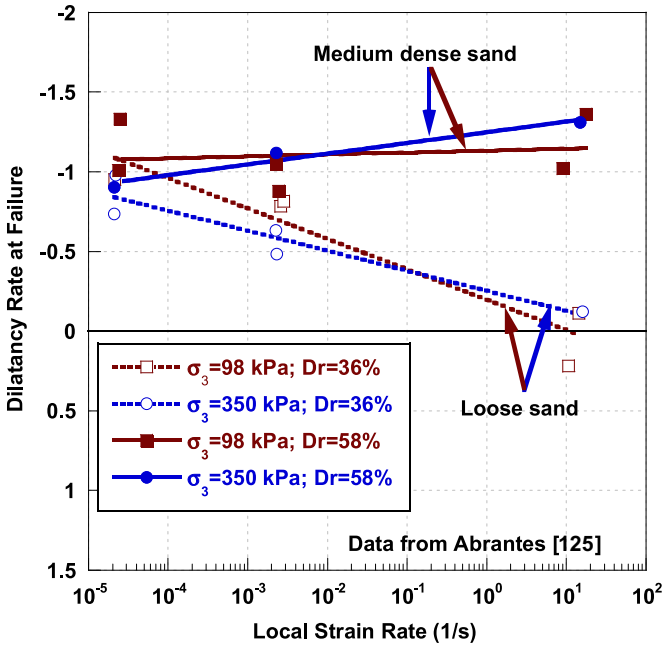

Fig. 22. Effect of HSR loading on dilatancy rate at failure of loose and medium sand.

If the decrease in pore pressure is large enough, or equivalently, if the tendency for dilation is high enough, the pore water pressure will reach zero at some point and the pore water will cavitate [21]. Consequently, there will be no further strength increase. This phenomenon occurs in medium dense and dense sand at low confining pressures where the tendency for dilation is highest. Holscher and Van Tol [12] and McManus and Davis [134] reported minimal increase in strength due to HSR loading of medium and dense sand under low confining pressures, with cavitation occurring in all tests.

Lee et al. [43] showed that at high confining pressures the behavior of dense saturated sand under HSR loading is primarily governed by grain crushing. The application of an HSR load to dense saturated sand under high confining pressure results in an unstable condition within the soil. There is a strong tendency for grain crushing in shear of dense sand under high confining pressure. However, under HSR loading, adequate time is given for grains to accumulate sufficient strain energy to fracture. After the termination of the HSR loading grains begin to crush with time, resulting in a progressive increase in pore pressure and an equivalent decrease in shear resistance, ultimately leading to failure. While there is clearly a need for better understanding of the HSR response of dense saturated sand at high confining pressures, progress will rely heavily on measurement of pore pressures within the sample, which is still considered to be a difficult task despite the advances in the field.

6.5. Modulus and strain to failure

Soil modulus is one of the most important parameters governing the response of soil to a propagating stress wave. Triaxial tests suggest that HSR loading generally increases the small strain modulus of sand, as indicated in Fig. 24. The modulus increase

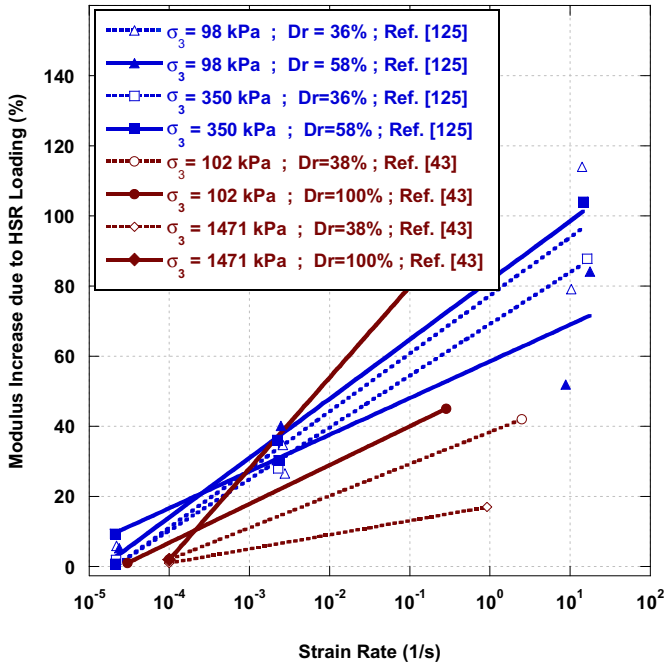

Fig. 24. Effect of HSR loading on modulus of dry sand in triaxial tests.

under HSR loading is greater in dense sand compared to loose sand, and is greatest at high confining pressures. It can therefore be concluded that the initial void ratio and confining pressure control the extent to which sand modulus is affected due to HSR loading. In addition to increasing the modulus, HSR loading also decreases the strain to failure by up to 2% [43,135]. The higher modulus and the lower strain to failure observed in HSR tests compared to quasi-static tests suggests that failure in HSR tests may be due to localization of shear deformations at strains corresponding to the peak, which in turn prevents further mobilization of shear resistance.

6.6. Shear band formation

Yamamuro and Abrantes [135] used imaging techniques to measure shear band inclination angles during HSR triaxial tests. They reported that while the Mohr-Coulomb theory approximates measured shear band inclinations closely at low strain rates of loading, under HSR loading the two measurements deviate by up to 10°. Recent numerical analyses also suggest a change in the orientation of the shear band in sand as strain rates increase [136,137]. These studies also suggest a change in thickness of the shear band with increasing strain rate.

Yamamuro et al. [138] suggested that peak stress in loose sands under HSR loading is associated with formation of shear bands. This is in contrast with the behavior of loose sand under low strain rates, in which shear bands form well past the peak and into the post peak region. It has been suggested that shear band formation in HSR loading occurs is a premature failure mechanism that prevents higher shearing resistance that would otherwise have mobilized. However, visualization of shear banding under HSR loading is difficult since shear bands originate within a soil sample and progress towards the exterior [134,139,140]. The time difference associated with onset of shear banding and visual indications on the exterior of a sample is considerably slower than the elastic wave propagation speed in sand, and is in the range of several milliseconds. This time difference becomes very significant under HSR loading. Shear bands may thus be visible at the surface later than they actually initiate within the sample. Observations of HSR response within the sample using flash X-ray [139–141] or recently developed transparent soil techniques [142–144], the latter of which is currently being employed by the authors, may provide further insight into onset and propagation characteristics of shear bands under HSR loading.

7. Shock wave tests

Although Shock tests are not traditionally employed to characterize typical soil parameters, they are useful in studying the behavior of soils at extremely high deformation rates and high stresses, such as those occurring in explosive loading. Shock wave tests are usually produced by impact of a flat plate on a target disc, which launches a planar shock wave into the sand target. A shock wave is characterized by a very steep stress wave front having very high amplitude, with pressures commonly in the range of 5–6 GPa. Deformation in a shock wave front is one-dimensional, thus representing confined compression. The strain rates are usually in excess of 10^5/s.

Simplified analysis of shock waves assumes that the shock wave amplitude is so high that the soil shows essentially no shear resistance to the propagating wave, thus allowing for shock equations from fluid dynamics to be applied (*e.g.* the use of pressure instead of principal stress). The simple form of shock equations is attributed to Rankine [145] and Hugoniot [146], and employs the equations for conservation of mass, momentum and energy as discussed by Meyers [22] and Kanel et al. [147]. These equations can be written in the following form:

$$\rho_0 U_S = \rho(U_S - U_P) \tag{3}$$

$$(P - P_0) = \rho_0 U_S U_P \tag{4}$$

$$E - E_0 = \frac{1}{2}(P + P_0)(V_0 - V) \tag{5}$$

where ρ, P, V, E denote density, pressure, specific volume (related to density), and energy behind the shock wave; ρ_0, P_0 and V_0 denote density, pressure, specific volume and energy in front of the shock wave; U_s and U_p are shock velocity and particle velocity, respectively. Eqs. (3-5) have five variables: P, U_p, U_s, V (or ρ) and E. In order to solve for one of the parameters in terms of the other four, an extra equation is introduced which relates U_s and U_p. This equation is known as the equation of state (EOS) of the material, and can be written in linear form for many solids as,

$$U_S = C_0 + SU_P \tag{6}$$

where C_0 is the speed of sound $C_0 = \sqrt{(K/\rho)}$, K is the bulk modulus of the material, and S is a constant defining the slope of the line. Parameters C_0 and S are experimentally determined, as shown in Fig. 25. The reader is referred to [22,147,148] for a detailed discussion of shock physics.

A range of C_0 values have been reported in the literature; the median is approximately 450 m/s, which implies a bulk modulus, K = 380 MPa. Comparing to the modulus computed from Fig. 7 (approximately 350 MPa for HSR loading), and ignoring the small difference between bulk modulus and constrained modulus, it can be seen that shock data are consistent with high rate uniaxial compression data.

A plot of Eq. (5) which describes the relationship between uniaxial stress and density is commonly known as the Hugoniot curve [22]. Analytically, the Hugoniot curve describes the locus of all the states that can be reached by shock compression [147]. One of the outcomes of shock studies in soils is to obtain the pressure at

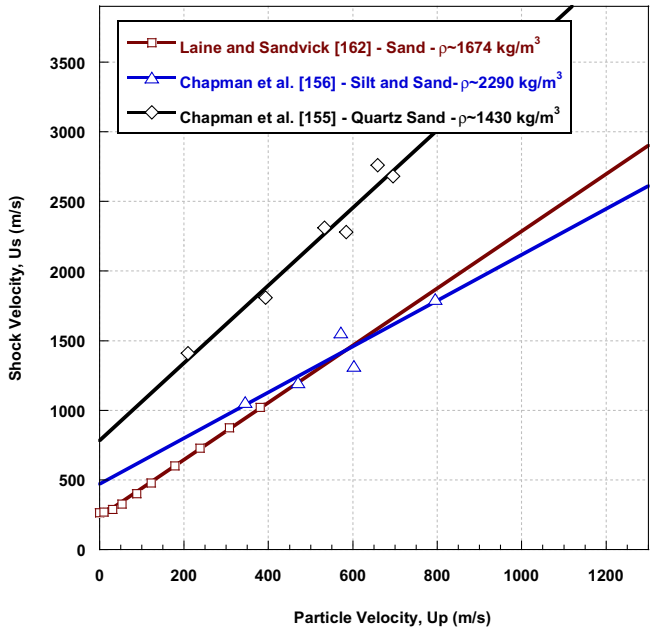

Fig. 25. Plot of shock velocity vs. particle velocity used to derive parameters of the equation of state (EOS).

which the sand is compacted to nearly the solid mineral phase density. At higher pressures the compressibility of silicate sand is assumed to be very similar to that of solid quartz (the constituent grain mineral). The EOS curve may also be expressed in terms of stress-density, and has been investigated by several authors for dry sand [18,149–160], as shown in Fig. 26. Chapman [155] found that water saturation up to 10% had no effect on shock compression.

As in the case of HSR uniaxial tests, shock experiments provide valuable information regarding stress-strain response of sand in uniaxial loading conditions. For example, shock compression of dry

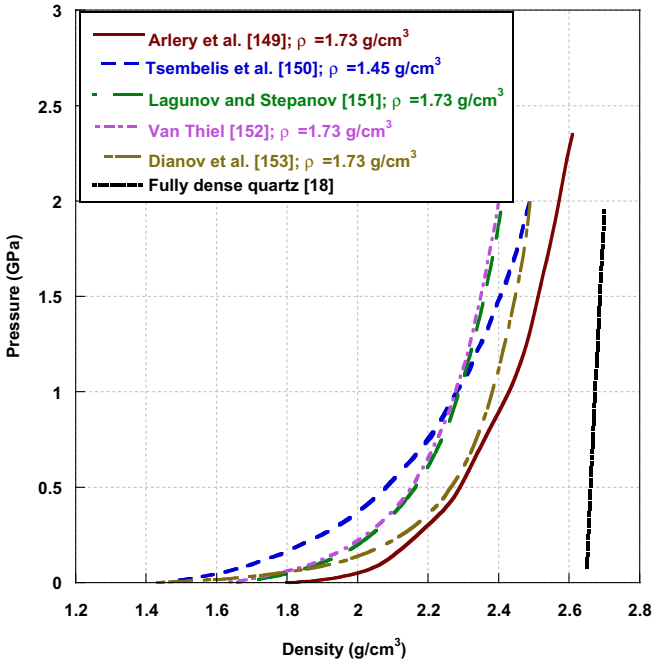

Fig. 26. Hugoniot compression states derived from shock tests on quartz sand.

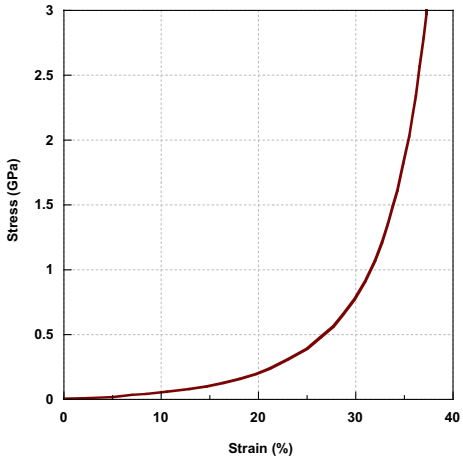

Fig. 27. Compaction curve of dry sand computed from Hugoniot data ($\rho 0 = 1.6$ g/cm3, $C = 0.45$ km/s, $S = 1.62$).

sand has yielded Hugoniot parameters averaging $C_0 = 0.45$ km/s and $S = 1.62$ (with U_p taken in units of km/s). These parameters can be used in conjunction with Eq. (6) to construct the stress-strain response of sand, shown in Fig. 27. The computed stress-strain response exhibits the locking response previously discussed for HSR uniaxial loading.

Shock tests typically provide data on uniaxial response. Vogler et al. [161] were recently able to generate shear waves along with longitudinal waves in the sample, allowing the characterization of soil behavior in shear as well as in uniaxial loading. Analysis of pressure-shear test results on very fine quartz sand presented by Vogler et al. [161] showed a sustained shear stress of approximately 180 MPa at a mean stress of approximately 150 MPa and a strain rate of nearly 3.5×10^4/s. Laine and Sandvik [162] suggested that the maximum shear strength of fully compacted sand can be taken approximately as the unconfined compressive strength of a reference rock with similar mineralogy. Lockner [163] in a review of rock strength data reports a mean strength of 210 MPa for quartzite, which approaches the maximum sustained shear stress reported by Vogler et al. [161] for fine grained quartz-based sand (Fig. 26). Therefore, pressure-shear tests may provide a useful tool for characterization of stress-strain response of sand at extremely high strain rates and high pressures in uniaxial loading as well as in shear.

8. Summary and conclusions

With respect to the behavior of sand under HSR loading, the following observations can be gleaned from published tests using uniaxial (confined) compression, SHPB, triaxial and shock tests:

- **Stiffness:** Although SHPB tests on dry sand show little increase in stiffness due to of HSR loading, uniaxial compression and triaxial tests exhibit a marked increase in stiffness due to HSR loading. The Dynamic modulus ratio in uniaxial compression tests increases gradually with increasing strain rate, with a ratio in excess of 2 reported for strain rates exceeding 10/s. Similarly, the dynamic modulus ratio of sand in triaxial shear increases up to twice the static value in dense sand under high confinement and HSR loading. The strain to peak decreases by up to 2% in HSR triaxial tests.
- **Strength:** The strength of sand measured under HSR loading depends on stress conditions within the sample, and is therefore a function of the testing method employed. Triaxial

compression tests have shown an increase of up to 30% in shear strength of dry sand as a result of HSR loading, with the effects being more pronounced in dense sand at high confining pressures. Limited data suggests that a change in the orientation of the failure surface by up to 10° under HSR loading may occur. Also, shock wave tests suggest that the strength of sand approaches that of the grain constituent mineral, at extreme high strain rates and pressures.

- **Confining pressure:** Triaxial SHPB tests performed at very high confining pressures in the range of 25–150 MPa indicate that strength increases with increasing confining pressure. It has also been observed that this relationship is not affected by increasing the loading strain rate. Quasi-static triaxial tests also indicate an increase in strength with increasing confining pressure. HSR Triaxial tests performed in the low confining pressure regime suggest that the dilatancy rate is affected by confining pressure. Accordingly, under low confining pressures in the range of 100 kPa the maximum dilatancy rate is not associated with failure, while at higher confining pressures the dilatancy rate is nearly maximum at peak shear strength, similar to static loading.
- **Saturation:** The response of saturated sand under HSR loading is essentially undrained, even if drainage is fully permitted. In triaxial tests fully saturated loose sand tends to expand and may exhibit very high increase in strength, due mainly to a decrease in pore pressures. Dense saturated sand expands under HSR loading, resulting in cavitation and showing limited effects on shear strength. HSR response of partially saturated sand in SHPB and uniaxial compression tests may be idealized as a bilinear response. An initial soft response is observed at strains below that required to bring the soil to a fully saturated state, while a stiff response results at higher strains associated with the fully saturated state.
- **Particle Breakage:** Limited data from SHPB and uniaxial compression tests suggest that particle breakage decreases with HSR loading. Available data suggests that particle breakage factor, B, decreases by up to 25% in HSR loading compared to static loading.

Some aspects of the HSR response of sand have not been fully covered in the literature, and may present avenues for future research. For example, the effect of strain rate on the failure mechanism under shear is not well understood. Similarly, the role of saturation should be investigated over a wide range of saturation degrees and strain rates under uniaxial compression and triaxial shear in order to assist in understanding the behavior of sand in a large number of practical problems. Additionally the effect of confining pressure, initial void ratio, particle shape, size, gradation, surface texture and mineralogy on particle breakage is useful in developing a comprehensive understanding of the response. Finally, all of the available data on the response of sand at high strain rates have been performed at the macro scale. The micromechanical response of sand due to HSR loading is believed to play an important role in explaining the behavior sand at the macro scale.

Acknowledgements

The authors gratefully acknowledge the support of the Defense Threat Reduction Agency (DTRA) Grant No: HDTRA1-10-1-0049 and National Science Foundation (NSF) grant DGE 0741714.

References

[1] Isenberg J. Nuclear geoplosics: part2, mechanical properties of earth materials. Defence Nuclear Agency; 1972. Report No. DNA 1285H2.
[2] Wang Z, Lu Y. Numerical analysis on dynamic deformation mechanism of soils under blast loading. Soil Dynamics and Earthquake Engineering 2003; 23:705–14.
[3] An J. Soil behavior under blast Loading. Ph.D. dissertation, University of Nebraska; N.E. 2010.
[4] Zhang JM. Transient shear strength of saturated sand under cyclic loading considering strain-rate effect. Soils and Foundations 1994;34(4):51–65.
[5] Kerley G. Numerical modeling of Buried mine explosions. Report ARL-CR-461. Army Research Laboratory; March 2001 [Unrestricted report available from the U.S. Department of Defense].
[6] Wang Z, Hao H, Lu Y. A three-phase soil model for simulating stress wave propagation due to blast loading. International Journal for Numerical and Analytical Methods in Geomechanics 2004;28:33–56.
[7] Grujicic M, Pandurangan B, Cheeseman BA, Roy WN, Skaggs RR. Parameterization of the porous material model for sand with different levels of water saturation. Soil Dynamics and Earthquake Engineering 2008;28:20–35.
[8] Anderson CE, Behner T, Weiss CE, Chocron S, Bigger RP. Mine blast loading: experiments and simulations. Southwest Research Institute; 2010. Report 18.12544/011.
[9] Theisen JG, Boyd WC, Crenshaw BM, Haisler JB. Analysis and modeling of soils Subjected to dynamic loading by aircraft Landing Gear. Proceedings of the International Symposium on wave propagation and dynamic properties of Earth materials, University of New Mexico, Albuquerque, New Mexico, August 23-25, 1967, pp. 335–348.
[10] Windisch EJ, Yong RN. The Determination of soil strain-rate behavior beneath a moving wheel. Journal of Terramechanics 1970;7(1):55–67.
[11] Gu Q, Lee FH. Ground response to dynamic compaction of dry sand. Geotechnique 2002;52(7):481–93.
[12] Holscher P, van Tol F. Rapid load testing on piles. Balkema: CRC Press, Taylor and Francis Group; 2009. p. 192.
[13] Stoffler D, Gault DE, Wedekind J, Polkowski G. Experimental hypervelocity impact into quartz sand: distribution and shock metamorphism of ejecta. Journal of Geophysical Research 1975;80(29):4062–77.
[14] Taylor T, Fragaszy RJ, Ho CL. Projectile penetration in granular soils. Journal of Geotechnical Engineering, ASCE 1991;117(4):658–72.
[15] Boguslavskii Y, Drabkin S, Juran I, Salman A. Theory and practice of projectile's penetration in soils. Journal of Geotechnical Engineering, ASCE 1996; 122(10):806–12.
[16] Field JE, Walley SM, Proud HT, Goldrein HT, Siviour CR. Review of experimental techniques for high rate deformation and shock studies. International Journal of Impact Engineering 2004;30(7):725–75.
[17] Chen WW, Song B. Split hopkinson (Kolsky) bar: design, testing and applications. Springer; 2011. p. 388.
[18] Brown JL, Vogler TJ, Chhabildaz LC, Reinhart WD, Thornhill TF. Shock response of dry sand. Albuquerque, N.M: Sandia National Laboratories; 2007. Report SAND2007–3524.
[19] Augustesen A, Liingaard M, Lade PV. Evaluation of time-dependent behavior of soils. International Journal of Geomechanics 2004;4(3):137–56.
[20] Liingaard M, Augustesen A, Lade PV. Characterization of models for time-dependent behavior of soils. International Journal of Geomechanics 2004; 4(3):157–77.
[21] Whitman RV. The response of soils to dynamic loading. Report No. 26, Final Report. Vicksburg, Mississippi: U.S. Army Engineer Waterways Experiment Station; 1970.
[22] Meyers MA. Dynamic behavior of materials. New York: Wiley; 1994.
[23] Hendron AJ. The behavior of sand in one-dimensional compression. Ph.D. dissertation, University of Illinois; Urbana, Illinois, 1963.
[24] Akers SA. Two-dimensional finite element analysis of porous geomaterials at multikilobar stress levels. Ph.D. dissertation, Virginia Polytechnic Institute and State University; Blacksburg, Virginia, 2001.
[25] de Beer EE. The scale effect in the transposition of the results of deep sounding tests on the ultimate bearing capacity of piles and caisson foundations. Geotechnique 1963;13(1):39–75.
[26] Whitman RV, Miller ET, Moore PJ. Yielding and locking of confined sand. Journal of the Soil Mechanics and Foundations Division, ASCE 1964;90(SM4): 57–84.
[27] Yamamuro JA, Bopp PA, Lade PV. One-Dimensional compression of sands at high pressures. Journal of Geotechnical Engineering, ASCE 1996;122(2):147–54.
[28] Bopp P. Effect of initial relative density on instability and behavior of granular materials at high pressure. PhD dissertation, Univerrsity of California, Los Angeles, C.A., 1994.
[29] Hagerty MM, Hite DR, Ullrich CR, Hagerty DJ. One-dimensional high-pressure compression of granular media. Journal of Geotechnical Engineering, ASCE 1993;119(1):1–18.
[30] Kolbuszewski J, Frederick MR. The significance of particle shape and size on the mechanical behavior of granular materials. European Conference on Soil Mechanics and Foundation engineering 1. 1963.
[31] Emerson MWC, Hendron AJ. Measurement of stress and strain during one dimensional compression of large compacted soil and Rockfill specimens; 1971. Contract Report S-71–4.
[32] Kjaernsli B, Sande A. Compressibility of some coarse-grained materials. Proceedings of Wiesbaden European Conference on Soil Mechanics and Foundation Engineering 1963;1:245–51.
[33] Horn HM, Deere DU. Frictional characteristics of minerals. Geotechnique 1962;12(4):319–35.

[34] Casagrande A. Characteristics of cohesionless soils affecting the stability of slopes and earth fills. Journal of Boston Society of Civil Engineers; 1936:257–76.
[35] Schofield A, Wroth P. Critical state soil mechanics. McGraw Hill; 1968. p. 310.
[36] Goh SH, Lee FH, Tan TS. Effects of lateral constraints and inertia on stress wave propagation in dry soil columns. Geotechnique 1999;48(4):449–63.
[37] Terzaghi K, Peck RB, Mesri G. Soil mechanics in engineering practice. 3rd ed. New York: John Wiley; 1996.
[38] Sadrekarimi A. Development of a new ring shear apparatus for investigating the critical state of sands. PhD dissertation, University of Illinois; Il, 2009.
[39] Rowe PW. Stress dilatancy relations for static equilibrium of an assembly of particles in contact. Proceedings of the Royal Society, Series A 1962;269: 500–27.
[40] Mitchell JK, Soga K. Fundamentals of soil behavior. 3rd Ed. John Wiley and Sons; 2005.
[41] Guo P, Su X. Shear strength, interparticle locking, and dilatancy of granular materials. Canadian Geotechnical Journal 2007;44:579–91.
[42] Sadrekarimi A, Olson SM. Critical state friction angle of sands. Geotechnique 2011;61(9):771–83.
[43] Lee KL, Seed, HB and Dunlop P. Effect of Transient Loading on the Strength of Sand. Proceedings of the 7th International Conference on Soil Mechanics and Foundation Engineering, vol. 1, Mexico City, Mexico, 1969. pp. 239–247.
[44] Lee KL, Seed HB. Drained strength characteristics of cohesionless soils. Berkeley, CA: Soil Mechanics and Bituminous Materials Research Laboratory, University of California; 1966.
[45] Lee KL, Seed HB. Drained strength characteristics of cohesionless soils. Journal of the Soil Mechanics and Foundations Division, ASCE 1967;93(SM6): 117–41.
[46] Vesic AS, Clough GW. Behavior of granular materials under high stresses. Journal of the Soil Mechanics and Foundations Division 1968;94(SM3): 661–88.
[47] Vesic AS, Barksdale RD. On shear strength of sand at very high pressures. ASTM Special Technical Publication; 1963. No. 361.
[48] Murphy DJ. Soils and rocks: composition, confining level and strength. PhD dissertation, Duke University; 1970.
[49] Hall, Gordon. Triaxial testing with large-scale pressure equipment laboratory shear testing of soils. ASTM Specialty Conference Technical Publication; 1963. No. 361, pp. 315–328.
[50] Bishop AW. Soil properties – Shear strength and consolidation. Panel Session, Proceedings of the Sixth International Conference on Soil Mechanics and Foundation Engineering. 1965.
[51] Marachi ND, Chan CK, Seed HB, Duncan JM. Strength and deformation characteristics of rockfill materials. Berkeley, CA: Department of Civil Engineering, University of California; 1969.
[52] Sadrekarimi A, Olson SM. Particle damage observed in ring shear tests on sands. Canadian Geotechnical Journal 2010;47(5):497–515.
[53] Billam J. Some aspects of the behavior of granular materials at high pressures. In: Parry RHG, Foulis GT, editors. Proceedings, Roscoe Memorial Symposium: stress-strain behavior of soils. UK: Cambridge; 1972. March 29-31, 1971.
[54] Lade PV, Yamamuro JA, Bopp PA. Significance of particle crushing in granular soils. Journal of Geotechnical Engineering, ASCE 1996;122(4):309–16.
[55] Nakata Y, Hyodo M, Hyde AFL, Kato Y, Murata H. Microscopic particle crushing of sand subjected to high pressure one-dimensional compression. Soils and Foundations 2001;41(1):69–82.
[56] McDowell GR, Bolton MD, Robertson D. The fractal crushing of granular materials. Journal of the Mechanics and Physics of Solids 1996;44(12): 2079–101.
[57] Rothenburg L, Kruyt NP. Critical state and evolution of coordination number in simulated granular materials. International Journal of Solids and Structures 2004;41:5763–74.
[58] McDowell GR, Bolton MD. On the micromechanics of crushable aggregates. Geotechnique 1998;48(5):667–79.
[59] Muir Wood D, Maeda K. Changing grading of soil: effect on critical states. Acta Geotechnica 2008;3:3–14.
[60] Li QM, Meng H. About the dynamic strength enhancement of concrete-like materials in a split hopkinson pressure bar test. International Journal of Solids and Structures 2003;40:343–60.
[61] Lee KL. Triaxial compressive strength of saturated sand under seismic loading conditions. Ph.D. dissertation, University of California; Berkeley, CA, 1965.
[62] Farr JV. Loading rate effects on the one-dimensional compressibility of four partially saturated soils. Technical Report SL-86-46. Vicksburg, MS: U.S. Army Engineer Waterways Experiment Station; 1986.
[63] Zaccor JV, Wallace NR. Techniques and equipment for determining dynamic properties of soils. California: United Research Services Corporation, Burlingame; 1963. DASA-1421, Final Report.
[64] Stoll RD, Ebeido IA. Shock waves in granular soils. Journal of Soil Mechanics and Foundations Division, ASCE 1965;91(SM4):107–25.
[65] Seaman L. One-Dimensional stress wave propagation in soils. DASA-1757. Menlo Park, California: Stanford Research Institute; 1966.
[66] Heierli W. Inelastic wave propagation in soil columns. Journal of Soil Mechanics and Foundation Division, ASCE 1962;88(SM6):33–63.
[67] Sparrow RW, Tory AC. Behavior of a soil mass under dynamic loading. Journal of Soil Mechanics Division, ASCE 1966;92(SM3):59–83.
[68] Schindler L. An Improved Facility for testing soils in one-dimensional compression. proceedings, International Symposium on wave propagation and dynamic properties of Earth materials, University of New Mexico, Albuquerque, N.M., 1967. pp. 847–860.
[69] Schindler, L. "Design and Evaluation of a device for determining the one-dimensional compression characteristics of soils subjected to impulse-type loads. PhD Thesis, University of Illinois, Urbana, Il., 1968.
[70] Farr JV, Woods RD. A device for evaluating one-dimensional compressive loading rate effects. Geotechnical Testing Journal, GTJODJ 1988;11(4): 269–75.
[71] Jackson JG, Ehrgott JQ, Rohani B. Loading rate effects on compressibility of sand. Miscellaneous paper SL-79-24. Vicksburg, Mi: U.S. Army Engineer Waterways Experiment Station; 1979.
[72] Jackson JG, Ehrgott JQ, Rohani B. Loading rate effects on compressibility of sand. Journal of the Geotechnical Engineering Division, ASCE, GT8; 1980:839–52.
[73] Whitman RV. The response of soils to dynamic loadings, report No. 17: stress-strain-time behavior of soil in one dimensional compression. Report No. 17. Vicksburg, Mississippi: U.S. Army Engineer Waterways Experiment Station; 1963.
[74] Akers SA. Uniaxial strain response of Enewetak Beach sand. Technical Report SL-86-45. Vicksburg, MS: U.S. Army Engineer Waterways Experiment Station; 1986.
[75] Roberts JE and de Souza JM. 1958. The compressibility of sands. ASTM Proceedings No. 58.
[76] McDowell GR, Harireche O. Discrete element modeling of soil particle fracture. Geotechnique 2002;52:131–5.
[77] Radhakrishnan N, Rohani B. A one-dimensional plane wave propagation code for layered nonlinear hysteretic media. Technical Report S-71-12. Vicksburg, Mi: U.S. Army Engineer Waterways Experiment Station; 1971.
[78] Hopkinson B. A method of measuring the pressure produced in the detonation of high explosives or by the impact of bullets. Philosophical Transactions of the Royal Society of London, Ser. A 1914;213:437–56.
[79] Kolsky H. An investigation of the mechanical properties of materials at very high rates of loading. Proceedings of the Royal Society of London, Ser. B 1949;62:676–700.
[80] Seaman L. Lagrangian analysis for multiple stress or velocity gages in attenuating waves. Journal of Applied Physics 1974;45(10):4304–14.
[81] Felice CW, Gaffney ES, Brown JA. Extended split-hopkinson bar analysis for attenuating materials. Journal of Engineering Mechanics, ASCE 1991;117(5): 1119–35.
[82] Kaiser MA. Advancements in split hopkinson bar test. Virginia Polytechnic Institute; MSc thesis, 1998.
[83] Felice CW. The response of soils to impulse loads using the split-hopkinson pressure bar technique, PhD thesis, University of Utah; 1985.
[84] Frew DJ, Forrestal MJ, Chen W. Pulse shaping techniques for testing brittle materials with a split hopkinson pressure bar. Experimental Mechanics 2002;42(1):93–106.
[85] Frew DJ, Forrestal MJ, Chen W. Pulse shaping techniques for testing elastic-plastic materials with a split hopkinson pressure bar. Experimental Mechanics 2005;45:186–95.
[86] Song B, Chen W, Luk V. Impact compressive response of dry sand. Mechanics of Materials 2009;41(6):777–85.
[87] Felice CW, Gaffney ES, Brown JA, Olsen JM. Dynamic high stress experiments on soil. Geotechnical Testing Journal GTJODJ 1987;10(4):192–202.
[88] Luo H, Lu WL, Komanduri R. Effect of mass density on the compressive behavior of dry sand under confinement at high strain rates. Experimental Mechanics; 2011. doi:10.1007/s11340-011-9475-2.
[89] Lu H, Luo H and Komaduri R. Dynamic compressive response of sand under confinements. Proceedings of the SEM Annual Conference, June 1–4, Albuquerque New Mexico, USA, p. 7. 2009.
[90] Bazhenov VG, Bragov AM, Kotov VL, Zefirov SV, Kochetkov AV, Krylov SV, et al. Analysis of the Applicability of a modified Kolsky's method for dynamic tests of soils in a deformable casing. Journal of Applied Mechanics and Technical Physics 2000;41(3):519–25.
[91] Bragov AM, Kotov VL, Lomunov, Sergeichev IV. Measurement of the dynamic characteristics of soft soils using the Kolsky's method. Journal of Applied Mechanics and Mechanical Physics 2004;45(4):580–5.
[92] Bragov AM, Lomunov AK, Sergeichev IV, Tsembelis K, Proud WG. Determination of physiomechanical properties of soft soils from medium to high strain rates. International Journal of Impact Engineering 2008;35: 967–76.
[93] Semblat JF, Luong MP, Gary G. 3D-Hopkinson bar: new experiments for dynamic testing on soils. Soils and Foundations 1999;39(1):1–10.
[94] Pierce SJ. High intensity compressive stress wave propagation through unsaturated sands. M.Sc. thesis, Colorado State University; Fort Collins, Co, 1989.
[95] Pierce SJ, Charlie WA. High-intensity compressive stress wave propagation through unsaturated sands. ESL-TR-90-12. Tyndall AFB, Fla: Air Force Engineering and Services Laboratory; 1990.
[96] Martin BE. Moisture effects on the high strain rate behavior of sand. M.Sc. thesis University of Florida, 2007.
[97] Kabir ME and Chen W. Sand particle breakage under high-pressure and high-rate loading. Dynamic Behavior of Materials, Volume 1, Conference

Proceedings of the Society for Experimental Mechanics Series 99, 2011, pp. 93–94.
[98] Kabir ME, Song B, Martin BE, Chen W. Compressive behavior of fine sand. SANDIA report, SAND2010–2289. New Mexico: Terminal Ballistics Technology Department, Sandia Laboratories; 2010.
[99] Murphy DJ. High pressure experiments on soil and rock. Proc. Thirteenth Symposium on Rock Mechanics, 1971. pp. 691–714.
[100] Lu YB, Li QM. About the dynamic uniaxial tensile strength of concrete-like materials. International Journal of Impact Engineering 2011;38:171–80.
[101] Marsal RJ. Large scale testing of rockfill materials. Journal of Soil Mechanics and Foundation Engineering Division, ASCE 1973;93(2):27–43.
[102] Lee KL, Farhoomand I. Compressibility and crushing of granular soil in anisotropic triaxial compression. Canadian Geotechnical Journal 1967;4(1): 68–86.
[103] Hardin BO. Crushing of soil particles. Journal of Geotechnical Engineering Division, ASCE 1982;111(10):1177–92.
[104] Lade PV, Yamamuro JA, Bopp PA. Significance of particle crushing in granular materials. Journal of Geotechnical Engineering 1996;122(4):309–16.
[105] Nakata Y, Hyde AFL, Hyodo M, Murata H. A Probabilistic approach to sand particle crushing in the triaxial test. Geotechnique 1999;49(5):567–83.
[106] Martin BE, Chen W, Song B, Akers SA. Moisture effects on high strain-rate behavior of sand. Mechanics of Materials 2009;41:786–98.
[107] Charlie WA, Ross CA, Pierce SJ. Split-Hopkinson pressure bar testing of unsaturated sand. Geotechnical Testing Journal GTJODJ 1990;13(6): 291–300.
[108] Veyera GE, Charlie WA, Hubert ME. One-Dimensional shock-induced pore pressure response in saturated carbonate sand. Geotechnical Testing Journal 2002;25(3):277–88.
[109] Whitman RV, Healy KA. Shear strength of sands during rapid loadings. Journal of Soil Mechanics and Foundations Division, ASCE 1962;88(SM2): 99–132.
[110] Thompson JB. Low-velocity impact penetration of low-cohesion soil deposits. Ph.D. dissertation, University of California; Berkeley, C.A., 1975.
[111] Savvateev AF, Budin AV, Kolikov VA, Rutberg PG. High-Speed penetration into sand. International Journal of Impact Engineering 2001;26: 675–81.
[112] Seed HB, Lundgren R. Investigation of the effect of transient loadings on the strength and deformation characteristics of saturated sands. Proceedings of the American Society of Testing and Materials 1954;54:1288–306.
[113] Whitman RV, Healy KA. The response of soils to dynamic loadings, report 9: shearing resistance of sands during rapid loadings. Report No. 9. Vicksburg, Mississippi: U.S. Army Engineer Waterways Experiment Station; 1962b.
[114] Huy NQ, van Tol AF, Holscher P. Laboratory investigation of the loading rate effects in sand; 2006. Report of TU-Delft, 24-08-2006.
[115] Schimming BB, Saxe HC. Inertial effects and soil strength criteria. Symposium on Soil-Structure Interaction, Engineering Research Lab., University of Arizona, Tucson, Arizona, September, 1964, pp. 118–128.
[116] Schimming BB, Haas HJ, Saxe HC. A comparison of the dynamic and static shear strengths of cohesionless, cohesive and combined soils. Technical Report No. AFWL TR-65-48. New Mexico: Air Force Weapons Laboratory, Kirtland Air Force Base; 1965.
[117] Whitman RV. The behavior of soils under transient loading. Proceedings, 4th International Conference on Soil Mechanics and Foundation Engineering, vol. 1, p. 207. 1957.
[118] Barnes GW. An investigation of the effect of dynamic loads on the shear strength of soils. M.Sc. thesis, Arizona State University; Tempe, Ariz. 1965.
[119] Vesic AS, Banks DC, Woodward JM. An experimental study of the dynamic bearing capacity of footings on sand. Proceedings, Sixth International Conference on Soil Mechanics and Foundation Engineering, vol. 2, pp. 209–213. 1965.
[120] Colp JL. An experimental investigation of the continuous penetration of a blunt body into a simulated cohesionless soil. Report SC-RR-65-260. Albuquerque, N.M: Sandia Corporation; 1965.
[121] Whitman RV and Luscher U. Footings for protective structures. Proceedings, SymposiuM on Protective Structures for Civilian Populations, National Academy of Sciences – National Research Council, Washington, D.C. 1965.
[122] Abrantes AE, Yamamuro JA. Experimental and data analysis techniques used for high strain rate tests on cohesionless soil. Geotechnical Testing Journal, GTJODJ 2002a;25(2):128–41.
[123] Abrantes AE and Yamamuro JA. Effect of strain rate in cohesionless soil. Proceedings of 15th ASCE Engineering Mechanics Conference, June 2-5, 2002, Columbia Univesity, New York, NY, 8 p. 2002b.
[124] Healy KA. The response of soils to dynamic loadings, report No. 13: the dependence of dilation in sand on the rate of shear strain. Report No. 13. Vicksburg, Mississippi: U.S. Army Engineer Waterways Experiment Station; 1963.
[125] Abrantes AE. Three dimensional stress-strain behavior of cohesionless material subjected to high strain rate. Ph.D. dissertation Clarkson University; 2003.
[126] Dwivedi SK, Teeter RD, Felice CW, Gupta YM. Two dimensional mesoscale simulations of projectile instability during penetration in dry sand. Journal of Applied Physics 2008;104. pp. 083502–1–10.
[127] Felice CW, Gupta YM. Penetration physics at the mesoscale. Report No. FA9950-06-0112. U.S. Air Force Office of Scientific Research; 2009.
[128] Addiss J, Collins A, Bodaru F, Promratana K, Proud WG. Dynamic behavior of granular materials at impact. Proceedings of DYMAT; 2009:59–65.
[129] Collins AL, Addiss JW, Walley SM, Promratana K, Bobaru F, Proud WG, et al. The effect of nose shape on the internal flow fields during ballistic penetration of sand. International Journal of Impact Engineering 2011;38: 951–63.
[130] Hardin B. Low-Stress dilation test. Journal of Geotechnical Engineering 1989; 115(6):769–87.
[131] Bolton MD. The strength and dilatancy of sand. Geotechnique 1986;36(1): 65–78.
[132] Karimpour H, Lade PV. Time effects relate to crushing in sand. Journal of Geotechnical and Geoenvironmental Engineering 2010;136(9):1209–19.
[133] Yamamuro JA, Lade PV. Effects of strain rate on instability of granular soils. Geotechnical Testing Journal, GTJODJ 1993;16(3):304–13.
[134] McManus KJ and Davis EO. (1996). Shear strength of dense sands during rapid loading. Proceedings of 7th Australia New Zealand Conference on Geomechanics: Geomechanics in Changing World, pp. 114–117.
[135] Yamamuro JA, Abrantes AE. Behavior of medium sand under very high strain rates. Geomechanics; Testing, Modeling, and Simulation: Proceedings of the First Japan-US Workshop on Testing, Modeling and Simulation, June 27-29, 2003, ASCE Geotechnical Special Publication, No. 143, pp. 61–70. 2003.
[136] Lemiale V, Muhlhaus HB, Meriaux C, Moresi L, Hodkinson L. Rate effects in dense granular materials: linear stability analysis and the fall of granular columns. International Journal for Numerical and Analytical Methods in Geomechanics 2011;35:293–308.
[137] Tejchman J, Wu W. FE-Investigation of shear localization in granular bodies under high shear rate. Granular Matter 2009;11:115–28.
[138] Yamamuro JA, Abrantes AE, Lade PV. Effect of strain rate on the stress. strain behavior of sand. Journal of Geotechnical and Geonvironmental Engineering 2011;137(12):1169–78.
[139] Alshibli KA, Sture S, Costes NC, Frank M, Lankton M, Batiste S, et al. Assessment of localized deformations in sand using x-ray computed tomography. ASTM Geotechnical Testing Journal 2000;23(3):274–99.
[140] Desrues J, Chambon R, Mokni M, Mazerolle F. Void ratio evolution inside shear bands in triaxial sand specimens studied by computed tomography. Geotechnique 1996;46(3):529–46.
[141] White DJ, Take WA, Bolton MD. Soil deformation measurement using particle image velocimetry (PIV) and photogrametry. Geotechnique 2003;53(7): 619–31.
[142] Iskander M. Modeling with transparent soils: visualizing soil-structure interaction and multi phase flow, non-intrusively. Springer Verlag; 2010.
[143] Liu J, Iskander MG. Modeling capacity of transparent soil. Cnadian Geotechnical Journal 2010;47(4):451–60.
[144] Iskander MG, Liu J. Spatial deformation measurement using transparent soil. Geotechnical Testing Journal, ASTM 2010;33(4):314–21.
[145] Rankine WJM. On the thermodynamic theory of waves of finite longitudinal disturbance. Philosophical Transactions of the Royal Society of London 1870; 160(1870):277–88.
[146] Hugoniot H. Propagation des Mouvements dans les Corps et spécialement dans les Gaz Parfaits (in French). Journal de l'Ecole Polytechnique 1887; 57(3).
[147] Kanel GI, Razorenov SV, Fortov VE. Shock-wave phenomena and the properties of condensed matter. Springer Verlag; 2004.
[148] Zukas JA, Theodore N, Swift HF, Greszczuk LB, Curran DR. Impact dynamics. New York: Wiley; 1982.
[149] Arlery M, Gardou M, Felureau JM, Mariotti C. Dynamic behavior of dry and water-saturated sand under planar shock conditions. International Journal of Impact Engineering 2010;37(1):1–10.
[150] Tsembelis K, Proud WG, Vaughan BM, Field JE. The behavior of sand under shock wave loading: experiments and simulations. 14–15 November 2002, (unpublished).
[151] Lagunov VA, Stepanov VA. Measurements of the dynamic compressibility of sand. Zhurnal Priklanoi Mekhaniki I Tehknichekoi Fiziki 1963;4:88–96.
[152] Van Thiel M, editor. Compendum of shock wave data. Lawrence Livermore Laboratory; 1977. Report UCRL-50108.
[153] Dianov M, Zlatin N, Mochalov S, Pugachev G, Rosomakho L. Shock compressibility of dry and water-saturated sand. Soviet Technical Physics Letters 1976;2:207–8.
[154] Cogar JR, Robinson N, Proud WG, Gross DLA. Shock Hugoniot data for low density silica powder. In: Furnish MD, Gupta YM, Forbes JW, editors. Shock Compression of Condensed Matter. American Institute of Physics; 2004.
[155] Chapman DJ, Tsembelis T, Proud EG. (2006a). The behavior of water saturated sand under shock loading. Proceedings of the 2006 SEM Annual Conference.
[156] Chapman DJ, Tsembelis K, Proud WG. (2006b). The behavior of dry sand under shock compression. Proceedings of Conference on Shock Compression of Condensed Matter-2005, American Institute of physics.
[157] Barker LM, Hollenbach RE. Shock-wave studies of PMMA, fused Silica, and sapphire. Journal of Applied Physics 1970;41:4208–26.
[158] Proud WG, Chapman DJ, Williamson DM, Tsembelis K, Addiss J, Bragov A, et al. The dynamic compaction of sand and related porous systems. CP955. In: Elert M, Furnish MD, Chau R, Holmes N, Nguyen J, editors. Shock Compression of Condensed Matter. American Institute of Physics; 2007. p. 1403–8.
[159] Resnyansky AD, Bourne NK. Shock-wave compression of a porous material. Journal of Applied Physics 2004;95:1760–70.
[160] Addiss J, Collins A, Bobaru F, Promratana K, Proud WG. Dynamic behavior of granular materials at impact. DYMAT; 2009:59–65.

[161] Vogler TJ, Alexander CS, Thornhill TF, Reinhart WD. Pressure-shear experiments on granular materials; 2011. Sandia Report SAND2011–6700.
[162] Laine L and Sandvik A. Derivation of mechanical properties for sand. Proceedings of the 4th Asia-Pacific Conference on Shock and Impact Loads on Structures, CI-Primer, PTE LTD, Singapore, 2001, pp. 361–368.
[163] Lockner DA. In: Ahrens T, editor. Rock failure, rock physics and phase relations. American Geophysical Union; 1995. p. 127–47.
[164] Fletcher EB, Poorooshasb HB. Response of a clay sample to low magnitude loads applied at high rate. Proceedings of the International Symposium on Wave Propagation and Dynamic Properties of Earth Materials, University of New Mexico Press, N.M., August 1968, pp. 781–786.
[165] Gaffney ES, Brown JA. Dynamic material properties for dry CARES alluvium. LA-UR-84-3795. Los Alamos, N.M: Los Alamos National Laboratory; 1984.
[166] Gaffney ES, Brown JA, Felice CW. Soils as samples for the split hopkinson bar. In 2nd Symposium on the Interaction of Non-Nuclear Mutations with Structures, Panama City Beach, Fl., April 15-18, 1985.
[167] Ross CA, Nash PT, Friesenhahn GJ. Pressure waves in soils using a split-hopkinson pressure bar. Report No. ESL-TR-86–29. Florida: Engineering & Services laboratory, Air Force Engineering and Service Center, Tyndall Air Force Base; 1986. 32403.
[168] Veyera GE. Uniaxial stress-strain behavior of unsaturated soils at high strain rates. WL-TR-93–3523. Tyndall AFB, FL: Wright Laboratory, Flight Dynamics Directorate; 1994.
[169] Semblat JF, Gary G, Luong MP. Dynamic response of sand using 3-Hopkinson bar. Proceedings of IS-Tokyo-95, first International Conference on Earthquake Geotechnical Engineering, Tokyo, 14–16 November, Balkema. 1995.
[170] Martin BE, Chen W. The high-rate behavior of a fine grain sand. Proceedings of the SEM Annual Conference, June 1–4 Albuquerque, N.M., 6 p. 2009.
[171] Kabir ME. Dynamic behavior of granular materials. PhD dissertation Purdue University; IN. 2010.
[172] Casagrande A, Shannon WL. Research on stress-deformation and strength characteristics of soils and soft rocks under transient loading. Soil Mechanics Series No. 31. Cambridge, Mass: Harvard University; 1948.
[173] Casagrande A, Shannon WL. Strength of soils under dynamic loads. Transactions, ASCE; 1949:755–73.
[174] Taylor DW, Whitman RV. The behavior of soils under dynamic loadings. Final report on laboratory studies. Report AFSWP-118. U.S. Armed Forces Special Weapons Project; 1954.
[175] Saxe HC, Graves LD, Stevason CC, Schimming BB, Drnevich VP, Kretschmer TR. Development of an apparatus for the dynamic direct shear testing of soils. Technical Documentary Report No. 63-3050. U.S: Air Force Weapons Lab; October 1963.
[176] Saxe HC, Graves LD, Schimming BB. Load-Time relationships in direct shear of soils. Highway Research Record, No. 48; January 1964. pp. 72–83.
[177] Schimming BB, Haas HJ, Saxe HC. A study of dynamic and static failure envelopes. Journal of Soil Mechanics and Foundations Division, ASCE 1966; 92(SM2):105–24.
[178] Carroll WF. A fast triaxial shear device. Geotechnical Testing Journal, GTJODJ 1988a;11(4):276–80.
[179] Carroll WF. Fast triaxial shear device evaluation. Technical report SL-88-2. Vicksburg, MS: U.S. Army Engineer Waterways Experiment Station; 1988b.
[180] Hendron AJ, Davisson MT, Parola JF. Effect of degree of saturation on compressibility of Suffield Experimental Station soils. Contract Report S-69-3. CE, Vicksburg, Mississippi: U. S. Army Engineer Waterways Experiment Station; 1969.
[181] Farr JV. On-dimensional loading-rate effects. Journal of Geotechnical Engineering 1990;116(1):119–35.